5.A. 5,6–diphenyl–1,2,4–triazine–3(2*H*)–ones bearing 5–substituted 1,3,4–oxadiazole [Series 1]

5.A.1. CHEMISTRY

Compounds **($S_1$4a-$S_1$4o)** were synthesised in four steps as per the reaction sequence outlined in **Scheme 4.1**. The initial two stages involved the synthesis of the 5,6-Diphenyl-1,2,4-triazin-3(2*H*)one framework **($S_1$1)** followed by its subsequent conversion into an acetohydrazide intermediate **($S_1$3)**. Intermediate **($S_1$2)** (Abdel Rahman *et al.*, 1994) was synthesised in appreciable yield (80%) by refluxing equimolar quantities of 5,6–Diphenyl–1,2,4–triazin–3(2*H*)–one **($S_1$1)** and ethyl chloroacetate in *N,N*–dimethylformamide (*N,N*–DMF) as a solvent. The key acetohydrazide intermediate **($S_1$3)** (Abdel Rahman *et al.*, 1994) was synthesised in appreciable yield (78%) by refluxing Ethyl 2–(3–oxo–5,6–diphenyl–1,2,4–triazin–2(3*H*)–yl)acetate **($S_1$2)** with hydrazine hydrate in absolute ethanol. The subsequent reaction of **($S_1$3)** with appropriate substituted aryl/heteroaryl acid derivatives in the presence of phosphorous oxychloride yielded the compounds **($S_1$4a–$S_1$4o)** *via* dehydration and cyclisation **(Table 5.1)**.

5.A.1.1. Physicochemical Characterisation

The R_f values were determined in solvent system n-hexane/ethyl acetate (1:1) to monitor the progress of the reaction. Subsequently, the percentage yield of the recrystallised final compounds was calculated which gave a fair idea regarding the reaction efficiency. It was followed by the determination of the melting point in open capillaries. Further, the Log P value of synthesised compounds was determined by octanol/water “shake-flask” method to establish

TABLE 5.1. Chemical Structures and Physicochemical Properties of Compounds **S$_1$4a-S$_1$4o**

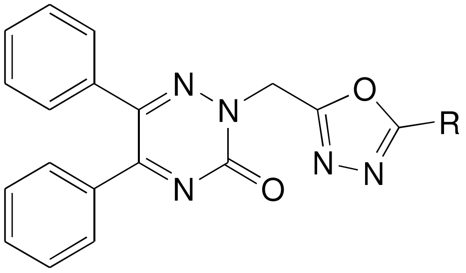

Compound	R	R$_f$$^{\#}$	% Yield	M.P. (°C)	Log P*
S$_1$4a	Phenyl	0.40	72	192-194	3.54
S$_1$4b	4-Methylphenyl	0.34	73	199-201	3.73
S$_1$4c	2-Methylphenyl	0.36	72	198-200	3.81
S$_1$4d	2,4-Dihydroxyphenyl	0.45	78	221-223	3.46
S$_1$4e	4-Aminophenyl	0.48	80	208-210	3.72
S$_1$4f	3-Chlorophenyl	0.45	78	214-216	3.82
S$_1$4g	4-Chlorophenyl	0.43	79	213-215	3.91
S$_1$4h	2,4-Dichlorophenyl	0.51	80	225-227	4.45
S$_1$4i	3-Methoxyphenyl	0.38	82	219-221	3.47
S$_1$4j	4-Methoxyphenyl	0.36	81	219-221	3.56
S$_1$4k	2-Nitrophenyl	0.35	78	230-232	3.64
S$_1$4l	4-Nitrophenyl	0.33	78	229-231	3.71
S$_1$4m	Pyridin-4-yl	0.43	70	201-203	3.67
S$_1$4n	3-Cyanophenyl	0.45	71	235-237	3.74
S$_1$4o	2,4-Dichlorophenoxy	0.47	77	233-235	4.40

$^{\#}$ Solvent system: n-hexane/ethyl acetate (1:1)

*Log P value was determined using shake flask method.

5.A.1.2. Spectral Characterisation and Elemental Analysis

The structures of compounds were characterised by FT–IR, ^{1}H NMR, ^{13}C distinct regions, *viz*, the biphenyls attached to the 1,2,4-triazine ring system, the methylene linkage between the 1,2,4-triazine and 1,3,4-oxadiazole nuclei, and the various substituted aromatic groups present at the fifth position of the 1,3,4–oxadiazole ring system. The signal of the methylene (–CH_2) protons was observed as a singlet around δ 4.22-3.50 ppm, a shift from its original base value of δ 1.30 ppm. This significant downfield shift confirmed its linkage to an aromatic/ heteroaromatic system that provided a deshielding effect.

The –OH and –NH_2 protons of **$S_1$4d** and **$S_1$4e** appeared as a singlet at δ 5.11 ppm and δ 4.12, respectively, and are D_2O exchangeable. The protons of the aromatic rings were observed as per the expected chemical shift. The structural assignment of all of the compounds was further supported by ^{13}C–NMR. The ^{13}C–NMR peaks of the 1,2,4–triazin–3(2*H*)–one nucleus appeared at 161.30-159.20 ppm (triazinone –C=O), and the –CH_2 peak appeared at approximately between 56.42-54.02 ppm. All other ^{13}C NMR peaks were seen as per the expected chemical shift. The results of the elemental analysis were within ±0.4% of the theoretical values.

Ethyl 2–(3–oxo–5,6–diphenyl–1,2,4–triazin–2(3*H*)–yl)acetate (S$_1$2)

Yield 80%; mp 142–144°C; R_f 0.35. FT-IR (KBr, cm^{-1}): 3061, 2987 ($C–H_{arom}$); 1743 ($C=O_{ester}$); 1674 ($C=O_{ketone}$); 1560 ($C=N_{triazine}$). ^1H NMR (300 MHz, DMSO–d_6): δ 7.43-7.23 (m, 10H, Ar–H); δ 4.19 (q, 2H, CH_2); δ 3.34 (s, 2H, CH_2CO); δ 1.22 (t, 3H, CH_3). ^{13}C NMR (75 MHz, DMSO–d_6): 167.26, 161.23, 153.37, 142.31, 135.73, 134.49, 131.19, 130.79, 129.47, 128.77, 127.99, 61.39, 54.28, 13.99. Anal. $C_{19}H_{17}N_3O_3$: C, 68.05; H, 5.11; N, 12.53%; Found: C, 67.87; H, 4.93; N, 12.51%.

Anal. $C_{17}H_{15}N_5O_2$: C, 63.54; H, 4.71; N, 21.79%; Found: C, 63.74; H, 4.69; N, 21.85%.

5,6–Diphenyl–2–((5–phenyl–1,3,4–oxadiazol–2–yl)methyl)–1,2,4–triazin–3(2*H*)-one (S₁4a)

FT-IR (KBr, cm^{-1}): 3059, 2524 (C–H$_{arom}$); 1678 (C=O$_{triazine}$); 1558 (C=N$_{triazine}$); 1180 (C–O–C$_{oxadiazole}$). ^{1}H NMR (300 MHz, DMSO–d_6): δ 7.92-7.12 (m, 15H, Ar–H); δ 4.18 (s, 2H, methylene). ^{13}C NMR (75 MHz, DMSO–d_6): 167.48, 160.00, 157.15, 153.86, 133.49, 132.31, 130.82, 129.63, 128.89, 126.60, 55.01. Anal. $C_{24}H_{17}N_5O_2$: C, 70.75; H, 4.21; N, 17.19%; Found: C, 71.03; H, 4.22; N, 17.22%.

5,6–Diphenyl–2–((5–p–tolyl–1,3,4–oxadiazol–2–yl)methyl)–1,2,4–triazin–3(2*H*)–one (S₁4b)

IR (KBr, cm^{-1}):3061, 2924 (C–H$_{arom}$); 1681 (C=O$_{triazine}$); 1552 (C=N$_{triazine}$); 1178 (C–O–C$_{oxadiazole}$). ^{1}H NMR (300 MHz, DMSO–d_6): δ 7.82-7.16 (m, 14H, Ar–H); δ 4.21 (s, 2H, methylene); δ 2.38 (s, 3H, methyl). ^{13}C NMR (75 MHz, DMSO–d_6): 165.10, 160.48, 157.02, 135.24, 134.94, 131.02, 130.10, 129.71, 128.61, 127.09, 126.73, 54.02, 21.91. Anal. $C_{25}H_{19}N_5O_2$: C, 71.25; H, 4.54; N, 16.62%; Found: C, 71.04; H, 4.55; N, 16.66%.

5,6–Diphenyl–2–((5–o–tolyl–1,3,4–oxadiazol–2–yl)methyl)–1,2,4–triazin–3(2*H*)–one (S₁4c)

FT-IR (KBr, cm^{-1}): 3078, 2934 (C–H$_{arom}$); 1680 (C=O$_{triazine}$); 1557 (C=N$_{triazine}$); 1172 (C–O–C$_{oxadiazole}$). ^{1}H NMR (DMSO–d_6): δ 7.77-7.13 (m, 14H, Ar–H); δ 4.22 (s, 2H, methylene); δ 2.35 (s, 3H, methyl). ^{13}C NMR (75 MHz, DMSO–d_6): 166.24, FT-IR (KBr, cm^{-1}): 3387, 3221 (–OH); 3070, 2926 ($C–H_{arom}$); 1693 ($C=O_{triazine}$); 1542 ($C=N_{triazine}$); 1128 ($C–O–C_{oxadiazole}$). ^1H NMR (300 MHz, DMSO–d_6): δ 7.45-6.83 (m, 13H, Ar–H); δ 5.11 (bs, 2H, –OH, D_2O exchangeable); δ 4.09 (s, 2H, methylene). ^{13}C NMR (75 MHz, DMSO–d_6): 167.36, 162.81, 160.98, 153.46, 142.39, 135.78, 134.54, 130.88, 129.52, 128.62, 127.01, 54.52. Anal. $C_{24}H_{17}N_5O_4$: C, 65.60; H, 3.90; N, 15.94%; Found: C, 65.75; H, 3.89; N, 15.98%.

2–((5–(4–Aminophenyl)–1,3,4–oxadiazol–2–yl)methyl)–5,6–diphenyl–1,2,4–triazin–3(2*H*)–one (S$_1$4e)

FT-IR (KBr, cm^{-1}): 3398 ($–NH_2$); 2926, 3061 ($C–H_{arom}$); 1604 ($C=O_{triazine}$); 1547 ($C=N_{triazine}$); 1180 ($C–O–C_{oxadiazole}$). ^1H NMR (300 MHz, DMSO–d_6): δ 7.50-7.00 (m, 14H, Ar–H); δ 4.12 (s, 2H, $–NH_2$, D_2O exchangeable); δ 3.50 (s, 2H, methylene). ^{13}C NMR (75 MHz, DMSO–d_6): 166.98, 160.35, 158.41, 156.05, 150.82, 143.83, 135.91, 130.37, 129.45, 128.51, 123.83, 118.19, 54.91. Anal. $C_{24}H_{18}N_6O_2$: C, 68.24; H, 4.29; N, 19.89%; Found: C, 67.99; H, 4.28; N, 19.82%.

2–((5–(3–Chlorophenyl)–1,3,4–oxadiazol–2–yl)methyl)–5,6–diphenyl–1,2,4–triazin–3(2*H*)–one (S$_1$4f)

FT-IR (KBr, cm^{-1}): 3074, 2918 ($C–H_{arom}$); 1695 ($C=O_{triazine}$); 1573 ($C=N_{triazine}$); 1141 ($C–O–C_{oxadiazole}$); 698 (C–Cl). ^1H NMR (300 MHz, DMSO–d_6): δ 7.90-7.27 (m, 14H, Ar–H); δ 4.06 (s, 2H, methylene). ^{13}C NMR (75 MHz, DMSO–d_6): 166.10, 161.02, 160.35, 151.34, 144.72, 142.32, 139.06, 138.81, 133.36, 132.90, 130.70, 128.88, 127.99, 55.02. Anal. $C_{24}H_{16}ClN_5O_2$: C, 65.24; H, 3.65; N, 15.85%; Found: C, 65.49; H, 3.66; N, 15.91%.

55.12. Anal. $C_{24}H_{16}ClN_5O_2$: C, 65.24; H, 3.65; N, 15.85%; Found: C, 65.42; H, 3.66; N, 15.87%.

2–((5–(2,4–Dichlorophenyl)–1,3,4–oxadiazol–2–yl)methyl)–5,6–diphenyl–1,2,4–triazin–3(*2H*)–one (S$_1$4h)

FT-IR (KBr, cm^{-1}): 3064, 2926 (C–H$_{arom}$); 1701 (C=O$_{triazine}$); 1554 (C=N$_{triazine}$); 1107 (C–O–C$_{oxadiazole}$); 771 (C–Cl). ^{1}H NMR (300 MHz, DMSO–*d$_6$*): δ 7.81-7.34 (m, 13H, Ar–H); δ 3.91 (s, 2H, methylene). ^{13}C NMR (75 MHz, DMSO–*d$_6$*): 165.79, 159.84, 142.13, 141.93, 136.52, 133.01, 132.35, 130.19, 129.27, 128.51, 127.98, 56.42. Anal. $C_{24}H_{15}Cl_2N_5O_2$: C, 60.52; H, 3.17; N, 14.70%; Found: C, 60.73; H, 3.18; N, 14.66%.

2–((5–(3–Methoxyphenyl)–1,3,4–oxadiazol–2–yl)methyl)–5,6–diphenyl–1,2,4–triazin–3(2*H*)–one (S$_1$4i)

FT-IR (KBr, cm^{-1}): 3061, 2928 (C–H$_{arom}$); 1683 (C=O$_{triazine}$); 1562 (C=N$_{triazine}$); 1180 (C–O–C$_{oxadiazole}$). ^{1}H NMR (300 MHz, DMSO–*d$_6$*): δ 7.89-6.76 (m, 14H, Ar–H); δ 3.86 (s, 3H, methoxy); δ 3.83 (s, 2H, methylene). ^{13}C NMR (75 MHz, DMSO–*d$_6$*): 167.09, 159.20, 153.37, 142.30, 135.72, 134.47, 132.16, 130.80, 129.68, 128.51, 127.99, 126.94, 121.52, 118.84, 113.88, 55.58, 55.29. Anal. $C_{24}H_{19}N_5O_3$: C, 68.64; H, 4.38; N, 16.01%; Found: C, 68.84; H, 4.37; N, 15.95%.

2–((5–(4–Methoxyphenyl)–1,3,4–oxadiazol–2–yl)methyl)–5,6–diphenyl–1,2,4–triazin–3(2*H*)–one (S$_1$4j)

FT-IR (KBr, cm^{-1}): 3059, 2939 (C–H$_{arom}$); 1683 (C=O$_{triazine}$); 1562 (C=N$_{triazine}$);

2–((5–(2–Nitrophenyl)–1,3,4–oxadiazol–2–yl)methyl)–5,6–diphenyl–1,2,4–triazin–3(2*H*)–one (S₁4k)

FT-IR (KBr, cm^{-1}): 3061, 2924 ($C–H_{arom}$); 1681 ($C=O_{triazine}$); 1562 ($C=N_{triazine}$); 1180 ($C–O–C_{oxadiazole}$); 1371 ($N–O_{nitro}$). ^1H NMR (300 MHz, DMSO–d_6): δ 8.13-7.25 (m, 14H, Ar–H); δ 4.02 (s, 2H, methylene). ^{13}C NMR (75 MHz, DMSO–d_6): 167.38, 160.27, 153.49, 142.44, 135.77, 134.53, 130.90, 129.58, 128.25, 127.01, 54.92. Anal. $C_{24}H_{16}N_6O_4$: C, 63.71; H, 3.56; N, 18.58%; Found: C, 63.52; H, 3.55; N, 18.63%.

2–((5–(4–Nitrophenyl)–1,3,4–oxadiazol–2–yl)methyl)–5,6–diphenyl–1,2,4–triazin–3(2*H*)–one (S₁4l)

FT-IR (KBr, cm^{-1}): 3113, 3061 ($C–H_{arom}$); 1695 ($C=O_{triazine}$); 1562 ($C=N_{triazine}$); 1180 ($C–O–C_{oxadiazole}$), 1346 ($N–O_{nitro}$). ^1H NMR (300 MHz, DMSO–d_6): δ 8.30-7.23 (m, 14H, Ar–H); δ 3.86 (s, 2H, methylene). ^{13}C NMR (75 MHz, DMSO–d_6): 166.14, 160.01, 150.29, 148.71, 136.59, 135.90, 134.65, 130.98, 129.55, 128.57, 124.00, 56.12. Anal. $C_{24}H_{16}N_6O_4$: C, 63.71; H, 3.56; N, 18.58%; Found: C, 63.93; H, 3.55; N, 18.53%.

5,6–Diphenyl–2–((5–(pyridin–4–yl)–1,3,4–oxadiazol–2–yl)methyl)–1,2,4–triazin–3(*2H*)–one (S₁4m)

FT-IR (KBr, cm^{-1}): 3061, 2928 ($C–H_{arom}$); 1676 ($C=O_{triazine}$); 1564 ($C=N_{triazine}$); 1180 ($C–O–C_{oxadiazole}$). ^1H NMR (300 MHz, DMSO–d_6): 8.21-7.78 (m, 4H, pyridyl–H); δ 7.76-7.05 (m, 10H, Ar–H); δ 3.89 (s, 2H, methylene). ^{13}C NMR (75 MHz, DMSO–d_6): 167.32, 161.30, 158.75, 156.91, 135.76, 134.44, 131.33, 130.85, 14H, Ar–H); δ 4.07 (s, 2H, methylene). ^{13}C NMR (75 MHz, DMSO–d_6): 167.29, 161.23, 153.39, 150.82, 142.33, 135.74, 134.50, 130.82, 129.31, 128.51, 126.96, 123.62, 115.90, 54.34. Anal. $C_{25}H_{16}N_6O_2$: C, 69.44; H, 3.73; N, 19.43%; Found: C, 69.18; H, 3.72; N, 19.49%.

2–((5–(2,4–Dichlorophenoxy)–1,3,4–oxadiazol–2–yl)methyl)–5,6–diphenyl–1,2,4–triazin–3(2*H*)–one (S$_1$4o)

FT-IR (KBr, cm^{-1}): 2924, 2854 (C–H$_{arom}$); 1658 (C=O$_{triazine}$); 1562 (C=N$_{triazine}$); 1080 (C–O–C$_{oxadiazole}$); 698, 763 (C–Cl). ^{1}H NMR (300 MHz, DMSO–d_6): δ 7.56-7.04 (m, 13H, Ar–H); δ 4.20 (s, 2H, methylene). ^{13}C NMR (75 MHz, DMSO–d_6): 167.25, 160.08, 153.34, 152.33, 142.29, 135.72, 134.47, 130.77, 129.26, 128.49, 127.98, 126.92, 124.77, 55.40. Anal. $C_{24}H_{15}Cl_2N_5O_3$: C, 58.55; H, 3.07; N, 14.23%; Found: C, 58.78; H, 3.08; N, 14.28%.

5.A.2. BIOLOGICAL ACTIVITY

5.A.2.1. Evaluation of Anti-Inflammatory Activity

5.A.2.1.1. Albumin Denaturation Assay

The albumin denaturation assay was performed to observe the preliminary anti-inflammatory potential of the synthesised compounds. The denaturation of tissue proteins and the subsequent production of auto-antigens is one of the well–documented causes of inflammatory and arthritic diseases (Opie, 1962; Umapathy *et al.*, 2010). Furthermore, NSAID's like indomethacin and celecoxib are reported to inhibit the denaturation of proteins (Grant *et al.*, 1970; Haque and Tauseef, 2016). Therefore, substances that can avert protein denaturation would be worthwhile for anti-inflammatory drug development since

Compounds **S$_{1}$4d, S$_{1}$4e, S$_{1}$4g, S$_{1}$4h, S$_{1}$4j, S$_{1}$4k, S$_{1}$4l** and **S$_{1}$4o**, exhibited appreciable inhibition of heat–induced protein (albumin) denaturation (67.71-80.81%) compared to standard indomethacin (84.88%).

TABLE 5.2. Albumin Denaturation Assay

Comp.	Absorbance	% Inhibition	Comp.	Absorbance	% Inhibition
Control	0.2137 ± 0.0170	––	**S$_{1}$4h**	0.3584 ± 0.0311[a]	67.71
Indo 10	0.3915 ± 0.0312[a]	84.88	**S$_{1}$4i**	0.3476 ± 0.0304[a]	62.66
S$_{1}$4a	0.3212 ± 0.0269[a]	50.30	**S$_{1}$4j**	0.3776 ± 0.0321[a]	76.70
S$_{1}$4b	0.3211 ± 0.0274[a]	50.26	**S$_{1}$4k**	0.3636 ± 0.0318[a]	70.14
S$_{1}$4c	0.3285 ± 0.0276[a]	53.72	**S$_{1}$4l**	0.3812 ± 0.0320[a]	78.38
S$_{1}$4d	0.3864 ± 0.0318[a]	80.81	**S$_{1}$4m**	0.3160 ± 0.0269[a]	47.87
S$_{1}$4e	0.3854 ± 0.0319[a]	80.35	**S$_{1}$4n**	0.3468 ± 0.0309[a]	62.28
S$_{1}$4f	0.3514 ± 0.0299[a]	64.44	**S$_{1}$4o**	0.3690 ± 0.0315[a]	72.67
S$_{1}$4g	0.3808 ± 0.0317[a]	78.19			

Values are expressed as the Mean ± S.D (n = 3); **a**: $p < 0.05$ vs. Control; **Indo 10:** Indomethacin 10 mg; All other compounds were taken at an equimolar oral dose relative to 10 mg indomethacin.

Compounds failing to elicit a minimum of 65% inhibition of protein denaturation compared to the "control" were dropped from the further evaluation process. The ability of the compounds to inhibit protein denaturation could be attributed to the formation of electrostatic forces and hydrophobic bonding, which are involved in the stabilisation of protein (albumin) against denaturation (Grant *et al.*, 1970).

5.A.2.1.2. Acute Oral Toxicity Studies

5.A.2.1.3. Carrageenan-Induced Rat Paw Oedema

The selected compounds **($S_1$4d, $S_1$4e, $S_1$4g, $S_1$4h, $S_1$4j, $S_1$4k, $S_1$4l** and **$S_1$4o)** were evaluated for carrageenan-induced rat paw oedema anti-inflammatory activity. The phlogistic agent carrageenan causes a severe inflammatory response apparent within 30 min when locally injected into the subplantar region of the rat paw.

Carrageenan-induced paw oedema resulted in a biphasic event, which mimics the exudative stage of inflammation, which is one of the critical processes of inflammatory pathology. The release of pro-inflammatory agents like histamine, serotonin occurs in the early phase (till 2 h); and the later stage (3 h post treatment) is associated with the activation of prostaglandins (Garcia *et al.*, 1973; Ozaki, 1990; Marzouk *et al.*, 2010). The result is summarised in **Table 5.3.** Mean changes in the paw oedema thickness at one-hour intervals from the induction of inflammation till six hours and the percentage inhibition of oedema were calculated and recorded. The results indicated that the compounds exhibited significant ($p < 0.05$) inhibition compared to the control.

The anti–inflammatory activity was after 4 h, where the time required for reaching the maximum activity, followed by a gradual decline is reported in **Table 5.3**. The maximum percentage inhibition was observed at 5 h and discussed accordingly. Indomethacin exhibited an inhibition of 62.64% against carrageenan-induced paw oedema at 5 h. In all eight evaluated derivatives, five were found to possess anti–inflammatory activity (55.25-59.07%).

Compound **$S_1$4d,** bearing a 2,4–dihydroxyphenyl group on the oxadiazole moiety, exhibited activity comparable (59.07%) to indomethacin. The oxadiazole nucleus bearing 4–amino phenyl **($S_1$4e)**, 4–chloro phenyl **($S_1$4g)**, 4–nitro phenyl

TABLE 5.3. Carrageenan-Induced Paw Oedema

Comp.	Swelling thickness in mm (% Inhibition)							Potency$^{\#}$
	0 h	1 h	2 h	3 h	4 h	5 h	6 h	
Control	3.69 ± 0.31	8.66 ± 0.71	8.86 ± 0.67	8.71 ± 0.69	8.62 ± 0.69	8.38 ± 0.74	8.13 ± 0.67	–
Indo 10	3.66 ± 0.30	3.67 ± 0.24^{a} (57.62)	3.59 ± 0.27^{a} (59.48)	3.44 ± 0.24^{a} (60.5)	3.35 ± 0.28^{a} (60.02)	3.22 ± 0.30^{a} (62.64)	3.43 ± 0.27^{a} (57.81)	100.0
$S_1$4d	3.64 ± 0.28	6.52 ± 0.57^{ab} (24.71)	4.92 ± 0.41^{ab} (44.47)	4.07 ± 0.33^{a} (53.27)	3.47 ± 0.23^{a} (59.74)	3.43 ± 0.23^{a} (59.07)	3.45 ± 0.28^{a} (57.56)	94.30
$S_1$4e	3.65 ± 0.29	6.58 ± 0.52^{ab} (24.02)	5.16 ± 0.40^{ab} (41.76)	4.19 ± 0.31^{ab} (51.89)	3.71 ± 0.25^{a} (56.96)	3.45 ± 0.27^{a} (58.83)	3.58 ± 0.28^{a} (55.96)	93.92
$S_1$4g	3.66 ± 0.25	6.67 ± 0.59^{ab} (22.98)	5.38 ± 0.42^{ab} (39.28)	4.24 ± 0.37^{ab} (51.32)	3.88 ± 0.22^{a} (54.99)	3.55 ± 0.26^{a} (57.64)	3.62 ± 0.27^{a} (55.47)	92.02
$S_1$4h	3.69 ± 0.28	7.62 ± 0.61^{ab} (12.01)	6.34 ± 0.54^{ab} (28.44)	5.99 ± 0.47^{ab} (31.23)	5.62 ± 0.42^{ab} (34.80)	5.17 ± 0.42^{ab} (38.31)	5.25 ± 0.43^{ab} (35.42)	61.16
$S_1$4j	3.71 ± 0.24	7.08 ± 0.59^{ab} (18.24)	5.43 ± 0.42^{ab} (38.71)	4.52 ± 0.31^{ab} (48.11)	4.08 ± 0.27^{ab} (52.67)	3.75 ± 0.28^{a} (55.25)	3.75 ± 0.31^{a} (52.71)	88.20
$S_1$4k	3.69 ± 0.24	7.61 ± 0.62^{a} (12.12)	6.14 ± 0.49^{ab} (30.70)	5.54 ± 0.38^{ab} (36.39)	5.28 ± 0.44^{ab} (38.75)	4.92 ± 0.33^{ab} (41.29)	4.96 ± 0.34^{ab} (39.00)	65.92
$S_1$4l	3.65 ± 0.26	6.93 ± 0.55^{ab} (19.98)	5.19± 0.42^{ab} (41.42)	4.39 ± 0.31^{ab} (49.60)	3.90± 0.27^{a} (54.76)	3.69 ± 0.27^{a} (55.96)	3.88± 0.25^{a} (52.27)	89.33
$S_1$4o	3.68 ± 0.22	7.31 ± 0.62^{ab} (15.59)	5.77 ± 0.40^{ab} (34.87)	5.05 ± 0.38^{ab} (42.02)	4.72 ± 0.34^{ab} (45.24)	4.43 ± 0.32^{ab} (47.14)	4.48 ± 0.32^{ab} (44.89)	75.25

Values are expressed as the Mean ± S.D (n = 6). **a**: $p < 0.05$ vs. Control; **b**: $p < 0.05$ vs. Indo 10; **Control:** 0.3% w/v sodium CMC in distilled water (10 ml/kg, *p.o.*); **Indo 10:** Indomethacin (10 mg/kg, *p.o*) in 0.3% w/v sodium CMC; All other compounds were administered in 0.3% w/v sodium CMC at an equimolar oral dose relative to 10 mg/kg indomethacin; # Potency was expressed as % oedema inhibition of the tested compounds relative to % oedema inhibition of Indo 10 “reference standard” at 5 h effect.

Thus, compounds **$S_1$4d, $S_1$4e, $S_1$4g, $S_1$4l** and **$S_1$4j** elicited promising anti–inflammatory activity of 94.30%, 93.92%, 92.02%, 89.33% and 88.20% potency relative to indomethacin at 5 h, thereby warranting further evaluation. It was observed that the substitution of the phenyl group attached to the oxadiazole ring with an electron-donating substituent such as a hydroxyl or amino group rendered a significant increase in activity (as seen in **$S_1$4d** and **$S_1$4e**) compared to electron-withdrawing substituents such as chloro, and nitro groups (**$S_1$4g,** and **$S_1$4l)**.

Based on the above observation and taking into cognizance the biphasic nature of carrageenan-induced paw oedema, it was possible to propose that the significant activity observed in the late phase of inflammation is attributed to the ability of the compounds to inhibit the release of late mediators. Thus, it is proposed that the evaluated compounds mitigate the inflammatory effects of carrageenan by inhibiting the release of prostaglandins.

5.A.2.1.4. Arachidonic Acid-Induced Rat Paw Oedema

The compounds **($S_1$4d, $S_1$4e, $S_1$4g, $S_1$4j** and **$S_1$4l)** were subjected for anti-inflammatory activity against arachidonic acid induced rat paw oedema to distinguish COX and LOX inhibition. Arachidonic acid (AA) induced paw oedema is used to distinguish between COX and lipoxygenase (LOX) inhibitors. This model is more sensitive to LOX than to COX inhibitors (Tsununi *et al.*, 1986). The paw oedema induced by AA is perceptibly reduced by inhibitors of AA metabolism and is insensitive to COX inhibitors (Di Martino *et al.*, 1987). The result of the arachidonic rat paw oedema bioassay is illustrated in **Table 5.4**.

The results showed that apart from zileuton (a selective LOX inhibitor),

TABLE 5.4. Arachidonic Acid Induced Paw Oedema

Compound	**Swelling thickness (mm)**	
	1 h	**% Inhibition**
Control	6.20 ± 0.49	–
ZIL 10	2.02 ± 0.12^{ab}	67.42
Indo 10	4.89 ± 0.31^{a}	21.13
$S_1$4d	5.01 ± 0.29^{ac}	19.19
$S_1$4e	5.18 ± 0.31^{ac}	16.45
$S_1$4g	5.11 ± 0.33^{ac}	17.58
$S_1$4j	5.35 ± 0.30^{ac}	13.71
$S_1$4l	5.44 ± 0.31^{ac}	12.26

Values are expressed as the Mean ± S.D (n = 6); **a**: $p < 0.05$ vs. Control; **b**: $p < 0.05$ vs. Indo 10; **c**: $p < 0.05$ vs. ZIL 10; **Control:** 0.3% w/v sodium CMC in distilled water (10 ml/kg, *p.o.*); **ZIL 10:** Zileuton (10 mg/kg, *p.o*) in 0.3% w/v sodium CMC; **Indo 10:** Indomethacin (10 mg/kg, *p.o*) in 0.3% w/v sodium CMC; All other compounds were administered in 0.3% w/v sodium CMC at an equimolar oral dose relative to 10 mg/kg indomethacin.

5.A.2.1.5. Cotton Pellet-Induced Granuloma in Rats

The selected compounds were evaluated for subchronic anti-inflammatory activity using cotton pellet induced granuloma method which has been extensively employed to assess the transudative, exudative and proliferative components of sub–chronic inflammation (Spector, 1969). The fluid absorbed by the pellet significantly influences the wet weight of the granuloma, and the dry weight correlates well with the amount of granulomatous tissue formed (Swingle and Shideman, 1972). Monocyte infiltration and fibroblast proliferation, rather than neutrophil infiltration and exudation, occur in sub–chronic inflammation (Dunne, 1990). The effects of the derivatives (**$S_1$4d, $S_1$4e, $S_1$4g, $S_1$4j, $S_1$4l)** and indomethacin on cotton pellet induced granuloma in rats is presented in **Table 5.5**. From the outcome, it can be inferred that the evaluated compounds and

TABLE 5.5. Cotton Pellet Induced Granuloma

Compound	Wt. of granulation (mg)
Control	94.13 ± 8.1
Indo 10	54.28 ± 4.2[a]
S_14d	56.11 ± 4.5[a]
S_14e	56.29 ± 4.2[a]
S_14g	57.80 ± 4.7[a]
S_14j	58.51 ± 5.3[a]
S_14l	58.07 ± 5.1[a]

Values are expressed as the Mean ± S.D (n = 6); **a**: $p < 0.05$ vs. Control; **Control:** 0.3% w/v sodium CMC in distilled water (10 ml/kg, *p.o.*); **Indo 10:** Indomethacin (10 mg/kg, *p.o*) in 0.3% w/v sodium CMC; All other compounds were administered in 0.3% w/v sodium CMC at an equimolar oral dose relative to 10 mg/kg indomethacin.

5.A.2.1.6. Freund's Adjuvant-Induced Arthritis in Rats

The compounds were further evaluated for chronic anti-inflammatory activity in Freund's adjuvant-induced arthritis model in rats as it is a fact that rheumatoid arthritis is a chronic destructive inflammatory polyarticular disease of the joints which is characterised by massive synovial proliferation and systemic and local inflammation causing cartilage and bone destruction. Adjuvant-induced arthritis in rats mimics many of the clinical and pathological features of human rheumatoid arthritis, such as paw swelling, joint erosion and ankylosis, and it is the most commonly used animal model for rheumatoid arthritis. Prostaglandins potentiate exudates by inducing the relaxation of arteriolar smooth muscle and increasing the blood supply to the tissue (Williams, 1979; Colpaert *et al.*, 1982; Oliver and Brahn, 1996).

Compounds **S_14d, S_14e, S_14g, S_14j** and **S_14l** as well as indomethacin were evaluated with respect to the control group in inhibiting Freund's adjuvant-

TABLE 5.6. Adjuvant-Induced Arthritis and Ulcer Index

Compound	Paw thickness (mm)							Ulcer Index
	Day 03	Day 06	Day 09	Day 12	Day 15	Day 18	Day 21	
Control	8.06 ± 0.73	8.11 ± 0.71	8.27 ± 0.73	8.21 ± 0.70	8.33 ± 0.68	8.41 ± 0.66	8.35 ± 0.70	0
Indo 10	5.39 ± 0.40[a] (33.13)	4.89 ± 0.36[a] (39.70)	4.76 ± 0.36[a] (42.44)	4.44 ± 0.32[a] (45.92)	4.06 ± 0.31[a] (51.26)	3.85 ± 0.27[a] (54.22)	3.61 ± 0.24[a] (56.77)	52 ± 5.9
$S_1$4d	5.54 ± 0.43[a] (31.26)	5.06 ± 0.37[a] (37.61)	4.94 ± 0.37[a] (40.27)	4.60 ± 0.32[a] (43.97)	4.18 ± 0.33[a] (49.82)	4.00 ± 0.30[a] (52.44)	3.82 ± 0.27[a] (54.25)	10 ± 1.4
$S_1$4e	5.55 ± 0.41[a] (31.14)	5.15 ± 0.41[a] (36.50)	4.90 ± 0.37[a] (40.75)	4.45 ± 0.34[a] (45.80)	4.34 ± 0.34[a] (47.90)	4.27 ± 0.30[a] (49.23)	3.99 ± 0.31[a] (52.21)	12 ± 1.8
$S_1$4g	5.64 ± 0.44[a] (30.02)	5.33 ± 0.41[a] (35.28)	4.96 ± 0.38[a] (40.02)	4.65 ± 0.35[a] (43.36)	4.51 ± 0.35[a] (45.86)	4.30 ± 0.31[a] (48.87)	4.01 ± 0.32[a] (51.98)	18 ± 1.9
$S_1$4j	5.64 ± 0.49[a] (30.02)	5.26 ± 0.42[a] (35.14)	5.06 ± 0.42[a] (38.81)	4.84 ± 0.33[a] (41.05)	4.71 ± 0.33[a] (43.46)	4.56 ± 0.30[ab] (45.78)	4.23 ± 0.31[a] (49.34)	11 ± 1.7
$S_1$4l	5.48 ± 0.50[a] (32.01)	5.18 ± 0.42[a] (36.13)	5.10 ± 0.43[a] (38.33)	5.78 ± 0.36[ab] (41.78)	4.68 ± 0.37[a] (43.82)	4.55 ± 0.35[a] (45.90)	4.20 ± 0.33[a] (49.70)	16 ± 1.1

Values are expressed as the Mean ± S.D (n = 6); **a**: $p < 0.05$ vs. Control; **b**: $p < 0.05$ vs. Indo 10; **Control:** 0.3% w/v sodium CMC in distilled water (10 ml/kg, *p.o.*); **Indo 10:** Indomethacin (10 mg/kg, *p.o*) in 0.3% w/v sodium CMC; All other compounds were administered in 0.3% w/v sodium CMC at an equimolar oral dose relative to 10 mg/kg indomethacin.

5.A.2.1.7. Evaluation of Ulcerogenic Liability

Compounds **(S$_1$4d, S$_1$4e, S$_1$4g, S$_1$4j** and **S$_1$4l)** exhibiting promising anti–inflammatory profiles were further assessed for their ulcerogenic liability regarding the ulcer index (UI) (Laloo *et al.*, 2013). The result of the ulcerogenic liability of sacrificed animals on the 21st day of post treatment with the standard drug and the test compounds in adjuvant-induced arthritis bioassay model is mentioned in **Table 5.6**.

The study revealed that all of the tested compounds exhibited superior gastrointestinal (GI) profiles (UI 10–18) in rats compared to standard indomethacin (UI 52). These findings, corroborated with the outcome of the histological evaluation of the gastric mucosa **(Fig. 5.1)**, further support the high gastric tolerability of the compounds relative to indomethacin.

5.A.2.1.8. Assessment of Hepatic and Renal Toxicity and Histopathology

Compounds (**S$_1$4d, S$_1$4e, S$_1$4g, S$_1$4j** and **S$_1$4l)** were further evaluated for hepatic and renal toxic liabilities through their effects on various liver and renal function parameters (serum enzymes, total protein and total albumin). The outcome of the estimation of various biochemical parameters (**Table 5.7**) confirms the safety of the compounds (**S$_1$4d, S$_1$4e, S$_1$4g, S$_1$4j** and **S$_1$4l**) compared to indomethacin for prolonged use. It is established by the histological studies of both the organs (**Fig. 5.2** and **Fig. 5.3**), which exhibit little necrosis or degeneration in the hepatocytes and nephrons, respectively, compared to the indomethacin-treated group.

TABLE 5.7. Effect of Selected Potential Compounds on Hepatic and Renal Toxicity Parameters as Evaluated on 21st Day after Treatment

Compound	SGOT (U/mL)	SGPT (U/mL)	Alkaline phosphatase (U/mL)	Total protein, g/dL	Total albumin, g/dL	Creatinine, mg/dL	Blood Urea Nitrogen, mg/dL
Control	92.48 ± 7.8	34.23 ± 2.5	17.82 ± 1.2	1.78 ± 0.11	1.77 ± 0.12	0.62 ± 0.049	23.48 ± 1.8
Indo 10	121.56 ± 9.8^{a}	52.83 ± 2.3^{a}	26.24 ± 1.1^{a}	2.24 ± 0.11^{a}	2.08 ± 0.15^{a}	1.84 ± 0.15^{a}	62.74 ± 5.4^{a}
$S_1$4d	99.35 ± 7.2^{a}	39.67 ± 1.9^{ab}	19.56 ± 0.8^{ab}	1.88 ± 0.09^{b}	1.82 ± 0.13^{b}	0.72 ± 0.065^{b}	38.67 ± 3.2^{ab}
$S_1$4e	98.21 ± 7.7 ^{b}	39.11 ± 2.2^{ab}	20.64 ± 0.9^{ab}	1.86 ± 0.07^{b}	1.87 ± 0.15	0.86 ± 0.078^{ab}	33.85 ± 2.7^{ab}
$S_1$4g	107.18 ± 8.1	42.45 ± 2.8^{ab}	20.28 ± 1.1^{ab}	1.91 ± 0.09^{b}	1.80 ± 0.11^{b}	0.78 ± 0.064^{ab}	42.28 ± 3.6^{ab}
$S_1$4j	103.17 ± 8.4^{b}	41.31 ± 2.4^{ab}	22.11 ± 0.7^{ab}	1.81 ± 0.05^{b}	1.87 ± 0.12	0.91 ± 0.080^{ab}	40.62 ± 3.2^{ab}
$S_1$4l	102.38 ± 7.8^{b}	45.28 ± 2.2^{ab}	19.92 ± 0.8^{ab}	1.84 ± 0.06^{b}	1.83 ± 0.13^{b}	0.88 ± 0.073^{ab}	39.24 ± 3.1^{ab}

SGOT: Serum Glutamic Oxaloacetic Transaminase; **SGPT:** Serum Glutamic Pyruvic Transaminase. Values are expressed as the Mean ± S.D (n = 6); **a**: $p < 0.05$ vs. Control; **b**: $p < 0.05$ vs. Indo 10; **Control:** 0.3% w/v sodium CMC in distilled water (10 ml/kg, *p.o.*); **Indo 10:** Indomethacin (10 mg/kg, *p.o*) in 0.3% w/v sodium CMC; All other compounds were administered in 0.3% w/v sodium CMC at an equimolar oral dose relative to 10 mg/kg indomethacin.

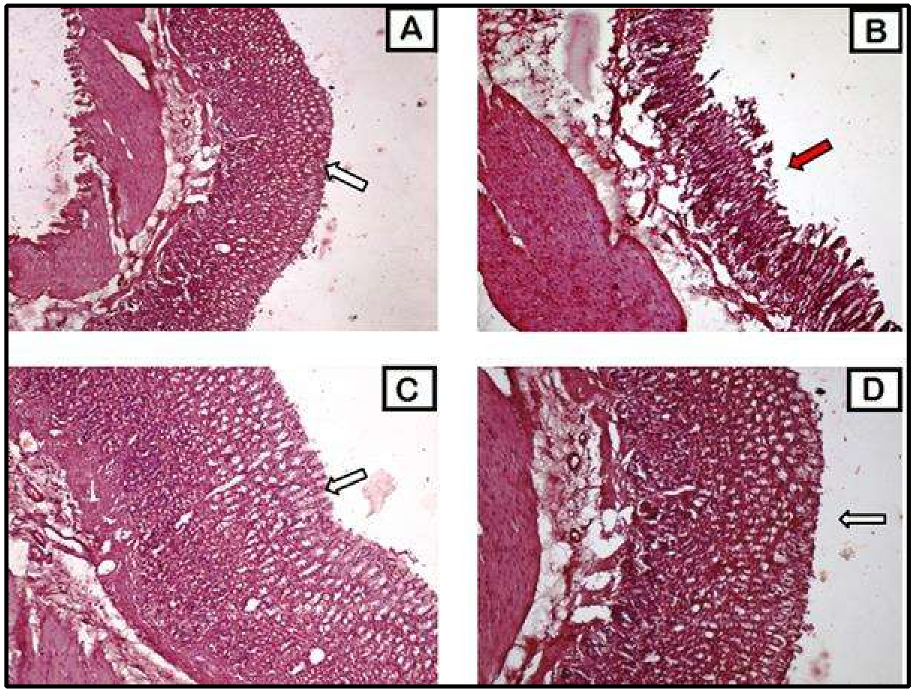

Figure 5.1. Photomicrographs (10x magnification) of **[A]** Control; **[B]** Indomethacin; **[C]** Compound **$S_1$4d** and **[D]** Compound **$S_1$4e** treated groups in rat stomach tissues (hematoxylin and eosin staining). The red arrow indicates severe detachment of surface epithelium, resulting in the formation of lesions. The White arrow indicates the typical stomach architecture with little or no ulcer formation.

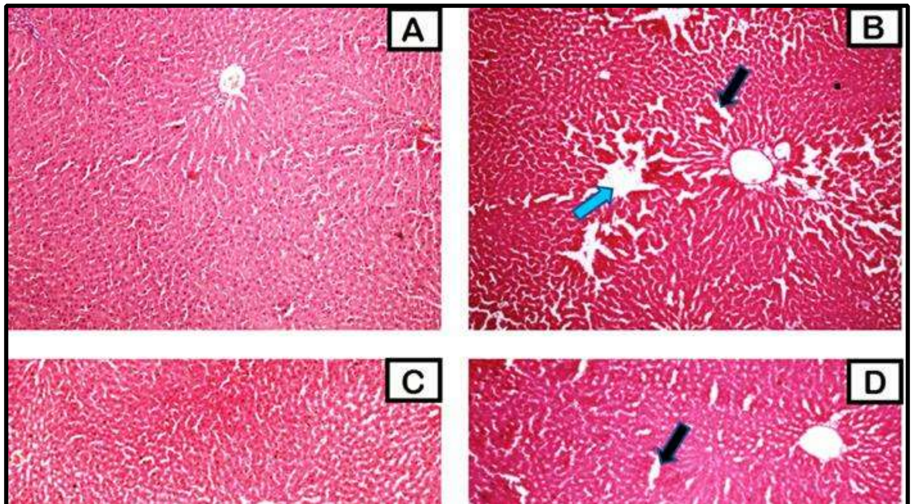

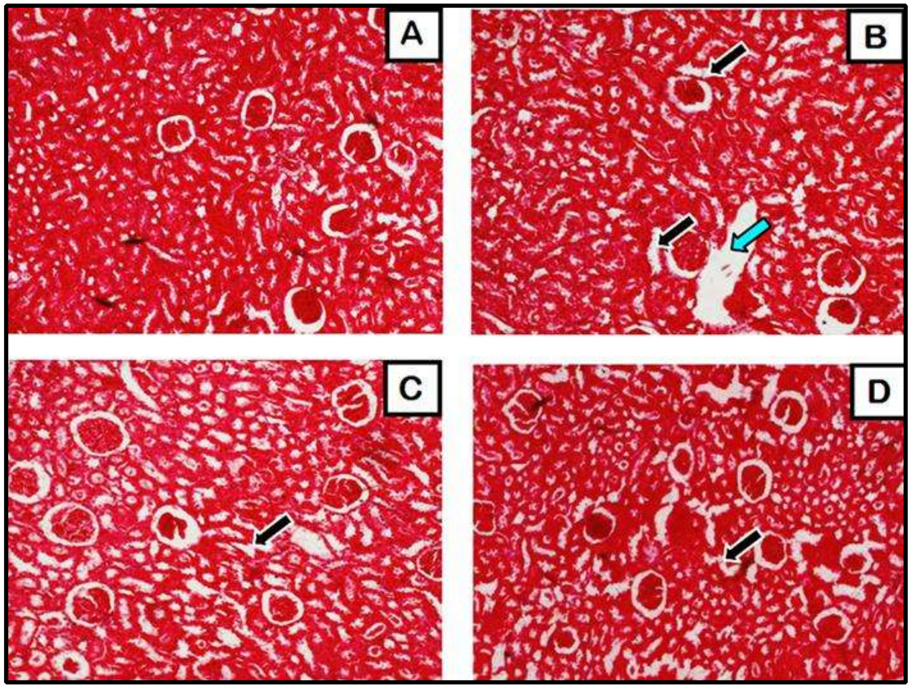

Figure 5.3. Photomicrographs (10x magnification) of **[A]** Control; **[B]** Indomethacin; **[C]** Compound **S₁4d** and **[D]** Compound **S₁4e** treated groups in rat kidney tissues (hematoxylin and eosin staining). Blue arrow indicates atrophy of renal tubule. Black arrows indicate mild tubular dilation of renal cortex and medulla.

5.A.2.2. Evaluation of Analgesic Activity

5.A.2.2.1. Acetic Acid-Induced Writhing in Mice

Acetic acid induces pain by increasing the levels of PGE_2 and $PGF_{2\alpha}$ at the peritoneal receptors (Deraedt *et al.*, 1980). It is postulated that acetic acid acts indirectly by inducing the release of endogenous mediators, which in turn stimulates the nociceptive neurons that are sensitive to NSAIDs and narcotics (Bentley *et al.*, 1983) (Collier *et al.*, 1968). The mechanism of the reaction to this nociceptive stimulus appears to be related to the prostanoid system.

The selected five compounds (**$S_1$4d, $S_1$4e, $S_1$4g, $S_1$4j** and **$S_1$4l)** along with

TABLE 5.8. Acetic Acid-Induced Writhing

Compound	Total no. of writhings	% Inhibition
Control	55.25 ± 3.90	--
Indo 10	12.55 ± 0.80[a]	77.28
$S_1$4d	15.25 ± 1.23[a]	72.40
$S_1$4e	15.55 ± 1.20[a]	71.85
$S_1$4g	14.77 ± 1.28[a]	73.26
$S_1$4j	16.46 ± 1.02[a]	70.21
$S_1$4l	13.90 ± 1.12[a]	74.84

Values are expressed as the Mean ± S.D (n = 6); **a**: $p < 0.05$ vs. Control; **Control:** 0.3 % w/v sodium CMC in distilled water (10 ml/kg, *p.o.*); **Indo 10:** Indomethacin (10 mg/kg, *p.o*) in 0.3% w/v sodium CMC; All other compounds were administered in 0.3% w/v sodium CMC at an equimolar oral dose relative to 10 mg/kg indomethacin.

Amongst the evaluated derivatives, compounds **$S_1$4g** and **$S_1$4l** exhibited the analgesic activity of 73.26% and 74.84% respectively, and that is comparable to the standard indomethacin (77.28%), as elicited by inhibiting the acetic acid induced abdominal constrictions and stretching in mice. Derivatives **$S_1$4d** (72.40%)**, $S_1$4e** (71.85%) and **$S_1$4j** (70.21%) exhibited moderate analgesic effects. The overall outcome of this test reiterated that the derivatives played a definitive role in the inhibition of prostaglandin (COX) biosynthesis, as evaluated from *in vivo* anti–inflammatory models (Dionne *et al.*, 2001).

5.A.2.2.2. Formalin-Induced Paw Licking in Mice

The formalin–induced pain test assesses the behavioural response to the injection of dilute formalin solution into the paw of an animal. This test is a useful model of clinical pain, defining two distinct periods of response, i.e., the equally, while peripherally acting drugs, such as indomethacin, inhibit the late phase (Tjolsen *et al.*, 1992). The compounds (**$S_1$4d, $S_1$4e, $S_1$4g, $S_1$4j** and **$S_1$4l**) were subjected to formalin-induced paw licking in mice for estimation of analgesic activity, and the result is summarised in **Table 5.9**.

TABLE 5.9. Formalin-Induced Paw Licking

Compound	**Time spent in licking (sec)**		**% Inhibition**	
	Phase I (0–10 min)	**Phase II (15–30 min)**	**Phase I (0–10 min)**	**Phase II (15–30 min)**
Control	114.60 ± 6.46	119.2 ± 8.31	–	–
Indo 10	96.67 ± 8.19	21.25 ± 1.28^{a}	15.64	82.17
PTZ 10	12.71 ± 0.41^{ab}	11.68 ± 0.53^{ab}	88.91	90.20
$S_1$4d	102.30 ± 6.62^{ac}	29.55 ± 2.25^{abc}	10.73	75.21
$S_1$4e	100.33 ± 5.82^{ac}	30.31 ± 1.38^{abc}	12.45	74.57
$S_1$4g	100.72 ± 5.57^{ac}	28.78 ± 1.42^{abc}	12.11	75.85
$S_1$4j	102.46 ± 6.71^{ac}	30.54 ± 2.57^{abc}	10.59	74.38
$S_1$4l	98.92 ± 8.24^{ac}	26.18 ± 1.38^{abc}	13.68	78.04

Values are expressed as the Mean ± S.D (n = 6); **a**: $p < 0.05$ vs. Control; **b**: $p < 0.05$ vs. Indo 10; **c**: $p < 0.05$ vs. PTZ 10; **Control:** 0.3% w/v sodium CMC in distilled water (10 ml/kg, *p.o.*); **Indo 10:** Indomethacin (10 mg/kg, *p.o*) in 0.3% w/v sodium CMC; **PTZ 10:** Pentazocine (10 mg/kg, *p.o*) in 0.3% w/v sodium CMC; All other compounds were administered in 0.3% w/v sodium CMC at an equimolar oral dose relative to 10 mg/kg indomethacin.

Pre-treatment of mice with derivatives at an equimolar oral dose relative to 10 mg/kg indomethacin failed to elicit significant effect during the early phase (0–10 min) but exhibited a significant effect in the second phase (15–30 min) of the bioassay model. The ability of the 1,2,4-triazine derivatives under evaluation to elicit an effect in the second phase confirms peripheral analgesic activity, *vitro* biochemical COX inhibitory assay. The result of the *in vitro* inhibition assay on both the isoforms of COX (COX-1 and COX-2) is presented in **Table 5.10**.

TABLE 5.10. COX Inhibitory Activity and Selectivity Index (COX–1/COX–2) of Selected Compounds

Comp.	IC_{50} (μM)[a]		COX–2 Selectivity index[b]	Type of Inhibition	COX–2 K_i (μM)
	COX–1	COX–2			
$S_1$4d	43.29 ± 2.203[f]	3.07 ± 0.219	14.10	competitive	14.51
$S_1$4e	43.39 ± 2.231[f]	3.10 ± 0.224	14.00	competitive	14.62
$S_1$4g	44.22 ± 2.277[f]	3.13 ± 0.251	14.13	competitive	14.71
$S_1$4j	44.93 ± 2.319[f]	3.23 ± 0.262	13.91	competitive	14.75
$S_1$4l	44.76 ± 2.668[f]	3.16 ± 0.260	14.16	competitive	14.79
Indo	3.74 ± 0.220	3.93 ± 2.221	0.95	competitive	9.86

Indo- Indomethacin; IC_{50} values are expressed as the Mean ± S.D; [a]Values acquired using an ovine COX assay kit (Catalog No. 760111, Cayman Chemical Inc., Ann Arbor, MI). Experiments were carried out in duplicate and had <10% error; [b]Selectivity for COX–2 is defined as IC_{50} (COX–1)/IC_{50} (COX–2); **f**: $p < 0.05$ vs. Indomethacin.

The results show that the tested compounds inhibited both the isoforms of the COX enzyme as the standard indomethacin to varying degrees. However, unlike indomethacin, they exhibited a preferential selectivity with a more than ten–fold preference towards the inhibition of COX–2 (IC_{50}: 3.07–3.23 μM) over COX–1 (IC_{50}: > 43 μM) enzyme. Compound **$S_1$4d** (IC_{50}: 3.07 μM) followed by compound **$S_1$4e** (IC_{50}: 3.10 μM) were the most potent preferential inhibitors of COX-2 within the series.

5.A.2.3.1. Enzyme Kinetics Study

A Lineweaver–Burk plot analysis was performed to examine the nature of

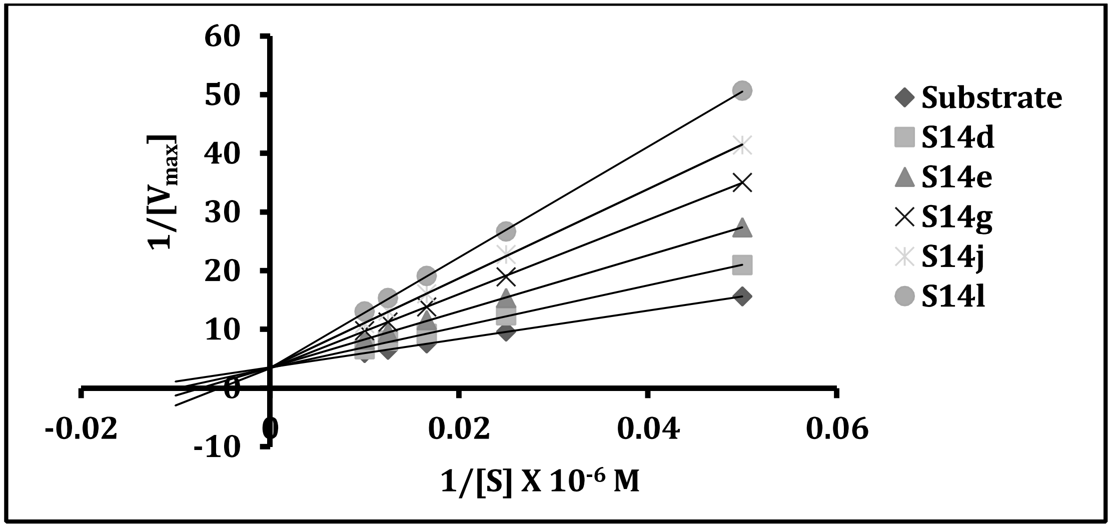

Figure 5.4. Lineweaver–Burk plot of *in vitro* COX–2 inhibition by potential derivatives of Series 1.

5.A.3. COMPUTATIONAL STUDIES

5.A.3.1. *In Silico* Docking

With an aim to rationalise the anti–inflammatory activity profile and taking into account the preferential binding with COX–2, a molecular docking study was undertaken by utilising the crystal structure of COX–2 (PDB ID: 1CX2) is depicted in **Fig. 5.5** and **Fig. 5.6**. It illustrates the binding interactions of the most potent compounds **S$_1$4d** and **S$_1$4e**within the COX–2 active site. The result of the docking study is depicted in **Table 5.11**.

Table 5.11. Glide Score and Docking Interactions of Selected Potential Compounds.

Sr. No.	Ligand	Glide Score	Amino acid interactions at the COX-2 active site
01	**S$_1$4d**	-9.05	His 90, Gln 192, Ser 353, Tyr 355, Leu 359, Arg 513, Asp 515, Phe 518, Val 523, Ala 527, Leu 531

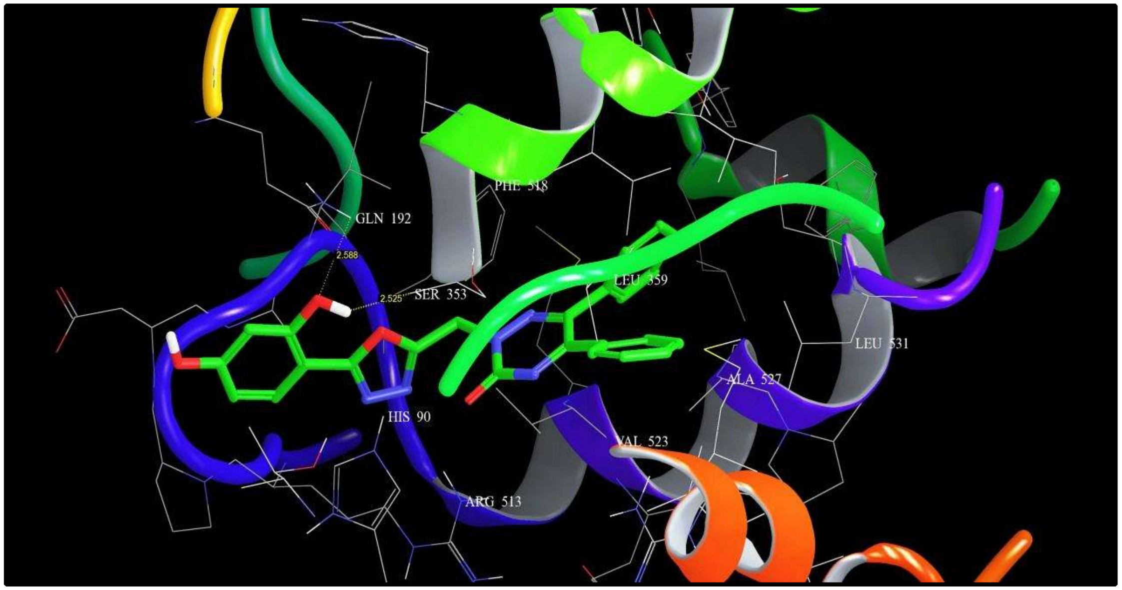

Figure 5.5. 3D view of the docking study of the minimum energy structure of the complex of **$S_1$4d** docked in COX–2 (PDB: 1CX2), viewed using the Glide XP visualizer of the Schrödinger Maestro 9.3 module.

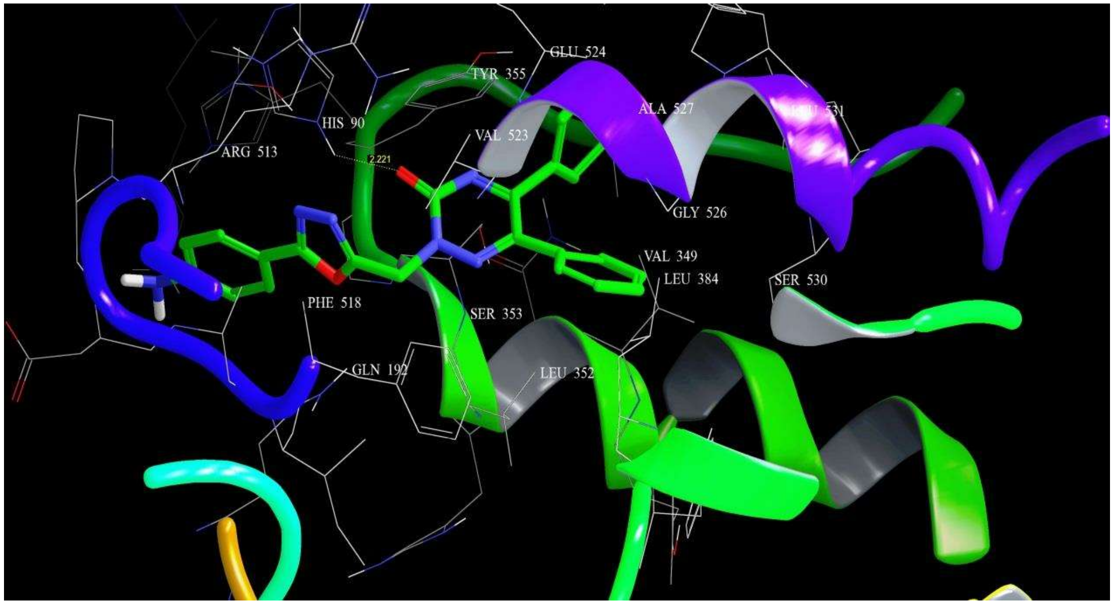

Figure 5.6. 3D view of the docking study of the minimum energy structure of the complex of **$S_1$4e** docked in COX–2 (PDB: 1CX2), viewed using the Glide XP visualizer of

523, Ser 353, Arg 513, Phe 518, Ala 527 and Leu 531 to name a few. The hydrophobic interactions of compounds **S$_1$4d** and **S$_1$4e** with the surrounding non–polar amino acid residues strongly contribute to the complex stabilisation, thereby translating into the compounds being effective inhibitors. The COX–2 active site constitutes a long hydrophobic channel along with areas of high electron density interacting with the aromatic ring system of NSAIDs. The biphenyls attached to the triazine nucleus in compounds **S$_1$4d** and **S$_1$4e** thus facilitate in anchoring the molecule deep within the COX–2 active pocket. This substantiates the role of lipophilicity as an important physicochemical parameter of a ligand for COX–2 inhibition.

5.A.3.2. *In silico* Molecular Dynamics (MD)

The interactions with the amino acids under *in silico* molecular dynamics study is illustrated in **Figs. 5.8** and **5.9**. The MD simulation of the energy-minimised docked complex of compound **S$_1$4d** with COX–2 was carried out to include implicit water molecules that participate in the dynamic hydrogen bonding with the polar amino acid residues present within the otherwise hydrophobic COX–2 active site. After the docking studies (**Table 5.11**), MD simulation was performed in an explicit aqueous solution environment. The overall stability of the system under simulation was evaluated using the root mean square deviations (RMSD) of the backbone atoms. The RMSD values of the backbone system computed against the structure of compound **S$_1$4d** is shown in **Fig. 5.7**.

The plot suggested that the RMSD of the protein backbone was stable over the course of the MD simulation and attained an equilibrium within 1.2 ns, with

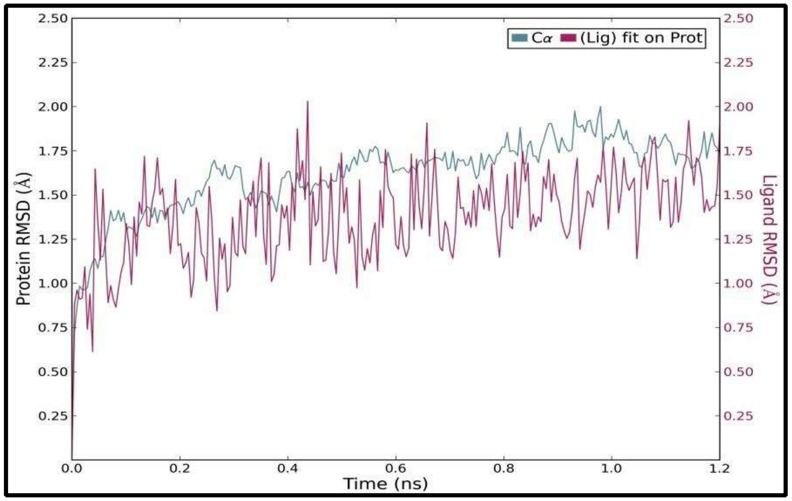

Figure 5.7. Protein–ligand RMSD. RMSD evaluation of protein (left *Y*–axis); the ligand RMSD (right *Y*–axis) indicates the stability of ligand **$S_1$4d** with respect to the protein and its binding pocket.

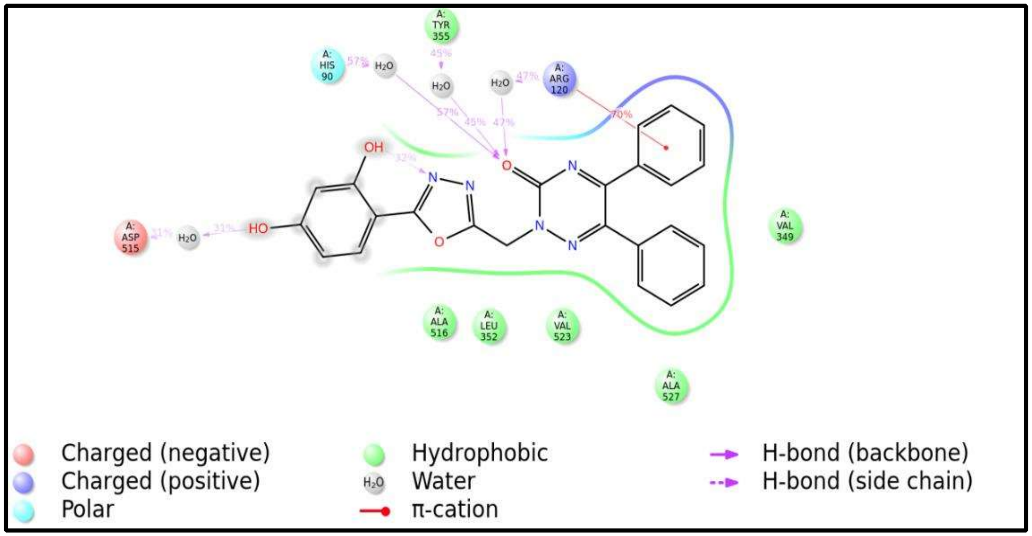

Figure 5.8. The detailed atomic interactions of ligand **$S_1$4d** with the key amino acid residues at the active site of COX–2.

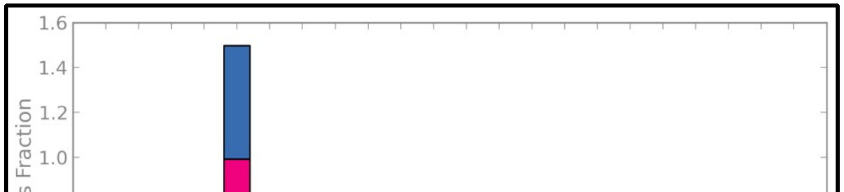

Thus, the compound **$S_1$4d** was seen to elicit anti–inflammatory activity through the modulation of key amino acid residues such as Tyr 355 and Arg 120 present within the active site in a manner similar to that reported for indomethacin (Cashman, 1996). The result of the MD study in **Fig. 5.9** presented the plot of protein interactions with compound **$S_1$4d** throughout the simulation.

The stacked bar charts were normalised over the course of the trajectory; for example, the value of 0.7 suggested that a specific interaction was maintained for 70% of the simulation time. The histogram thus helped in assessing the role of each of the specific bonds with the active amino acid residues, which significantly contributed to the overall stabilisation of the protein-ligand complex. Thus, MD simulation was effectively utilised to understand the role of the active site hydration that prevails under normal physiological conditions in the better interpretation of the biological profile.

5.A.3.3. Estimation of "Drug-Like" Properties

The "drug-likeliness" of the most active compounds **$S_1$4d, $S_1$4e, $S_1$4g, $S_1$4j** and **$S_1$4l** was assessed by calculating their agreement with Lipinski's rule of five (Lipinski *et al.*, 2001). The result is summarised in **Table 5.12**. This approach has been routinely used as a filter for substances that have the potential to be further developed in drug design programs. This rule is based on the observation that most orally administered drugs have a molecular weight ≤ 500, a log P ≤ 5, hydrogen bond donor sites ≤ 5 and hydrogen bond acceptor sites (N and O atoms) ≤ 10. Also, the total polar surface area (TPSA) was also calculated, as it is another key property linked to drug bioavailability. Thus, passively absorbed molecules with a TPSA > 140 are considered to possess low oral bioavailability

TABLE 5.12. Calculated Lipinski's Rule of Five for the Most Active Compounds

Compound	Parameters					[f]*N* violations
	[a]Log P	[b]TPSA	[c]MW	[d]nON	[e]nOHNH	
$S_1$4d	3.46	127.17	439.43	9	2	0
$S_1$4e	3.72	112.74	422.45	8	2	0
$S_1$4g	3.91	86.71	441.88	7	0	0
$S_1$4j	3.56	95.95	437.46	8	2	0
$S_1$4l	3.71	132.54	452.43	10	0	0

[a]Data was taken from **TABLE 5.1;** [b]Total Polar Surface Area; [c]Molecular Weight; [d]No. of hydrogen bond acceptors; [e]No. of hydrogen bond donors; [f]No. of violations of Lipinski's rule.

The outcome of this exercise indicated that all of the synthesised compounds complied with these rules and showed no violation. Theoretically, these compounds should present good passive oral absorption, and differences in their bioactivity cannot be solely attributed to the above-predicted values.

TABLE 5.3. Carrageenan-Induced Paw Oedema

Comp.	**Swelling thickness in mm (% Inhibition)**							**Potency#**
	0 h	**1 h**	**2 h**	**3 h**	**4 h**	**5 h**	**6 h**	
Control	3.69 ± 0.31	8.66 ± 0.71	8.86 ± 0.67	8.71 ± 0.69	8.62 ± 0.69	8.38 ± 0.74	8.13 ± 0.67	–
Indo 10	3.66 ± 0.30	3.67 ± 0.24[a] (57.62)	3.59 ± 0.27[a] (59.48)	3.44 ± 0.24[a] (60.5)	3.35 ± 0.28[a] (60.02)	3.22 ± 0.30[a] (62.64)	3.43 ± 0.27[a] (57.81)	100.0
S$_1$4d	3.64 ± 0.28	6.52 ± 0.57[ab] (24.71)	4.92 ± 0.41[ab] (44.47)	4.07 ± 0.33[a] (53.27)	3.47 ± 0.23[a] (59.74)	3.43 ± 0.23[a] (59.07)	3.45 ± 0.28[a] (57.56)	94.30
S$_1$4e	3.65 ± 0.29	6.58 ± 0.52[ab] (24.02)	5.16 ± 0.40[ab] (41.76)	4.19 ± 0.31[ab] (51.89)	3.71 ± 0.25[a] (56.96)	3.45 ± 0.27[a] (58.83)	3.58 ± 0.28[a] (55.96)	93.92
S$_1$4g	3.66 ± 0.25	6.67 ± 0.59[ab] (22.98)	5.38 ± 0.42[ab] (39.28)	4.24 ± 0.37[ab] (51.32)	3.88 ± 0.22[a] (54.99)	3.55 ± 0.26[a] (57.64)	3.62 ± 0.27[a] (55.47)	92.02
S$_1$4h	3.69 ± 0.28	7.62 ± 0.61[ab] (12.01)	6.34 ± 0.54[ab] (28.44)	5.99 ± 0.47[ab] (31.23)	5.62 ± 0.42[ab] (34.80)	5.17 ± 0.42[ab] (38.31)	5.25 ± 0.43[ab] (35.42)	61.16
S$_1$4j	3.71 ± 0.24	7.08 ± 0.59[ab] (18.24)	5.43 ± 0.42[ab] (38.71)	4.52 ± 0.31[ab] (48.11)	4.08 ± 0.27[ab] (52.67)	3.75 ± 0.28[a] (55.25)	3.75 ± 0.31[a] (52.71)	88.20
S$_1$4k	3.69 ± 0.24	7.61 ± 0.62[a] (12.12)	6.14 ± 0.49[ab] (30.70)	5.54 ± 0.38[ab] (36.39)	5.28 ± 0.44[ab] (38.75)	4.92 ± 0.33[ab] (41.29)	4.96 ± 0.34[ab] (39.00)	65.92
S$_1$4l	3.65 ± 0.26	6.93 ± 0.55[ab] (19.98)	5.19± 0.42[ab] (41.42)	4.39 ± 0.31[ab] (49.60)	3.90± 0.27[a] (54.76)	3.69 ± 0.27[a] (55.96)	3.88± 0.25[a] (52.27)	89.33
S$_1$4o	3.68 ± 0.22	7.31 ± 0.62[ab] (15.59)	5.77 ± 0.40[ab] (34.87)	5.05 ± 0.38[ab] (42.02)	4.72 ± 0.34[ab] (45.24)	4.43 ± 0.32[ab] (47.14)	4.48 ± 0.32[ab] (44.89)	75.25

Values are expressed as the Mean ± S.D (n = 6). **a**: $p < 0.05$ vs. Control; **b**: $p < 0.05$ vs. Indo 10; **Control:** 0.3% w/v sodium CMC in distilled water (10 ml/kg, *p.o.*); **Indo 10:** Indomethacin (10 mg/kg, *p.o*) in 0.3% w/v sodium CMC; All other compounds were administered in 0.3% w/v sodium CMC at an equimolar oral dose relative to 10 mg/kg indomethacin; # Potency was expressed as % oedema inhibition of the tested compounds relative to % oedema inhibition of Indo 10 “reference standard” at 5 h effect.

TABLE 5.6. Adjuvant-Induced Arthritis and Ulcer Index

Compound	Paw thickness (mm)							Ulcer Index
	Day 03	Day 06	Day 09	Day 12	Day 15	Day 18	Day 21	
Control	8.06 ± 0.73	8.11 ± 0.71	8.27 ± 0.73	8.21 ± 0.70	8.33 ± 0.68	8.41 ± 0.66	8.35 ± 0.70	0
Indo 10	5.39 ± 0.40^{a} (33.13)	4.89 ± 0.36^{a} (39.70)	4.76 ± 0.36^{a} (42.44)	4.44 ± 0.32^{a} (45.92)	4.06 ± 0.31^{a} (51.26)	3.85 ± 0.27^{a} (54.22)	3.61 ± 0.24^{a} (56.77)	52 ± 5.9
$S_1$4d	5.54 ± 0.43^{a} (31.26)	5.06 ± 0.37^{a} (37.61)	4.94 ± 0.37^{a} (40.27)	4.60 ± 0.32^{a} (43.97)	4.18 ± 0.33^{a} (49.82)	4.00 ± 0.30^{a} (52.44)	3.82 ± 0.27^{a} (54.25)	10 ± 1.4
$S_1$4e	5.55 ± 0.41^{a} (31.14)	5.15 ± 0.41^{a} (36.50)	4.90 ± 0.37^{a} (40.75)	4.45 ± 0.34^{a} (45.80)	4.34 ± 0.34^{a} (47.90)	4.27 ± 0.30^{a} (49.23)	3.99 ± 0.31^{a} (52.21)	12 ± 1.8
$S_1$4g	5.64 ± 0.44^{a} (30.02)	5.33 ± 0.41^{a} (35.28)	4.96 ± 0.38^{a} (40.02)	4.65 ± 0.35^{a} (43.36)	4.51 ± 0.35^{a} (45.86)	4.30 ± 0.31^{a} (48.87)	4.01 ± 0.32^{a} (51.98)	18 ± 1.9
$S_1$4j	5.64 ± 0.49^{a} (30.02)	5.26 ± 0.42^{a} (35.14)	5.06 ± 0.42^{a} (38.81)	4.84 ± 0.33^{a} (41.05)	4.71 ± 0.33^{a} (43.46)	4.56 ± 0.30^{ab} (45.78)	4.23 ± 0.31^{a} (49.34)	11 ± 1.7
$S_1$4l	5.48 ± 0.50^{a} (32.01)	5.18 ± 0.42^{a} (36.13)	5.10 ± 0.43^{a} (38.33)	5.78 ± 0.36^{ab} (41.78)	4.68 ± 0.37^{a} (43.82)	4.55 ± 0.35^{a} (45.90)	4.20 ± 0.33^{a} (49.70)	16 ± 1.1

Values are expressed as the Mean ± S.D (n = 6); **a**: $p < 0.05$ vs. Control; **b**: $p < 0.05$ vs. Indo 10; **Control:** 0.3% w/v sodium CMC in distilled water (10 ml/kg, *p.o.*); **Indo 10:** Indomethacin (10 mg/kg, *p.o*) in 0.3% w/v sodium CMC; All other compounds were administered in 0.3% w/v sodium CMC at an equimolar oral dose relative to 10 mg/kg indomethacin.

TABLE 5.7. Effect of Selected Potential Compounds on Hepatic and Renal Toxicity Parameters as Evaluated on 21st Day after Treatment

Compound	**SGOT (U/mL)**	**SGPT (U/mL)**	**Alkaline phosphatase (U/mL)**	**Total protein, g/dL**	**Total albumin, g/dL**	**Creatinine, mg/dL**	**Blood Urea Nitrogen, mg/dL**
Control	92.48 ± 7.8	34.23 ± 2.5	17.82 ± 1.2	1.78 ± 0.11	1.77 ± 0.12	0.62 ± 0.049	23.48 ± 1.8
Indo 10	121.56 ± 9.8[a]	52.83 ± 2.3[a]	26.24 ± 1.1[a]	2.24 ± 0.11[a]	2.08 ± 0.15[a]	1.84 ± 0.15[a]	62.74 ± 5.4[a]
$S_1$4d	99.35 ± 7.2[a]	39.67 ± 1.9[ab]	19.56 ± 0.8[ab]	1.88 ± 0.09[b]	1.82 ± 0.13[b]	0.72 ± 0.065[b]	38.67 ± 3.2[ab]
$S_1$4e	98.21 ± 7.7[b]	39.11 ± 2.2[ab]	20.64 ± 0.9[ab]	1.86 ± 0.07[b]	1.87 ± 0.15	0.86 ± 0.078[ab]	33.85 ± 2.7[ab]
$S_1$4g	107.18 ± 8.1	42.45 ± 2.8[ab]	20.28 ± 1.1[ab]	1.91 ± 0.09[b]	1.80 ± 0.11[b]	0.78 ± 0.064[ab]	42.28 ± 3.6[ab]
$S_1$4j	103.17 ± 8.4[b]	41.31 ± 2.4[ab]	22.11 ± 0.7[ab]	1.81 ± 0.05[b]	1.87 ± 0.12	0.91 ± 0.080[ab]	40.62 ± 3.2[ab]
$S_1$4l	102.38 ± 7.8[b]	45.28 ± 2.2[ab]	19.92 ± 0.8[ab]	1.84 ± 0.06[b]	1.83 ± 0.13[b]	0.88 ± 0.073[ab]	39.24 ± 3.1[ab]

SGOT: Serum Glutamic Oxaloacetic Transaminase; **SGPT:** Serum Glutamic Pyruvic Transaminase. Values are expressed as the Mean ± S.D (n = 6); **a**: $p < 0.05$ vs. Control; **b**: $p < 0.05$ vs. Indo 10; **Control:** 0.3% w/v sodium CMC in distilled water (10 ml/kg, *p.o.*); **Indo 10:** Indomethacin (10 mg/kg, *p.o*) in 0.3% w/v sodium CMC; All other compounds were administered in 0.3% w/v sodium CMC at an equimolar oral dose relative to 10 mg/kg indomethacin.

5.B. 5,6-diphenyl-1,2,4-triazine-3(2*H*)-ones bearing five-member (1,3,4-oxadiazole/thiadiazole, 1,2,4-triazole) heterocyclic moieties [Series 2]

5.B.1. CHEMISTRY

The target compounds were synthesised in two steps process from a common precursor from Series 1, 2-(3-Oxo-5,6-diphenyl-1,2,4-triazin-2(3*H*)-yl) acetohydrazide **($S_1$3)** as per the reaction sequence outlined in **Scheme 4.2**. Reaction of **($S_1$3)** with various aryl isothiocyanates in ethanol yielded the corresponding aryl thiosemicarbazides **($S_2$1a-$S_2$1e)**.

The thiosemicarbazides **($S_2$1a-$S_2$1e)** were oxidatively cyclised to 5-arylamino-1,3,4-oxadiazole compounds **($S_2$2a-$S_2$2e)** by the elimination of hydrogen sulphide using iodine and potassium iodide in ethanolic NaOH. The 5-arylamino-1,3,4-thiadiazole compounds **($S_2$3a-$S_2$3e)** were obtained by cyclisation of **($S_2$1a-$S_2$1e)** after treating it with cold concentrated sulphuric acid. Lastly, the thiosemicarbazides **($S_2$1a-$S_2$1e)** on heating with ethanolic 4 N NaOH underwent cyclisation through dehydration to afford the 1-aryl-5-mercapto-1,2,4-triazole compounds **($S_2$4a-$S_2$4e)**.

5.B.1.1. Physicochemical Characterisation

The R_f values were determined in solvent system DCM/methanol (9.5:0.5) to monitor the progress of the reaction. Subsequently, the percentage yield of the recrystallised final compounds was calculated which gave a fair idea regarding the reaction efficiency. This was followed by the determination of the melting point in open capillaries. Further, the Log P values of synthesised compounds were determined by octanol/water "shake-flask" method to establish

TABLE 5.13. Chemical Structures and Physicochemical Properties of Compounds **$S_2$2a-$S_2$2e; $S_2$3a-$S_2$3e; $S_2$4a-$S_2$4e**

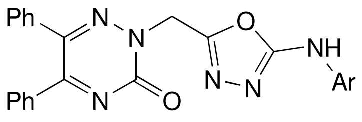

($S_2$2a-$S_2$2e)

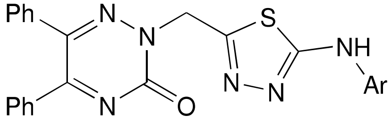

($S_2$3a-$S_2$3e)

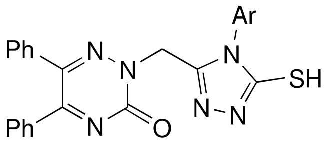

($S_2$4a-$S_2$4e)

Compound	Ar	R_f#	% Yield	M.P. (°C)	Log P*
$S_2$2a	Phenyl	0.40	69	229-231	3.44
$S_2$2b	4-Methylphenyl	0.39	71	235-237	3.98
$S_2$2c	4-Methoxyphenyl	0.35	76	246-248	4.00
$S_2$2d	4-Chlorophenyl	0.33	80	244-245	4.19
$S_2$2e	4-Nitrophenyl	0.45	79	255-257	3.89
$S_2$3a	Phenyl	0.39	70	232-233	4.32
$S_2$3b	4-Methylphenyl	0.42	74	240-242	4.45
$S_2$3c	4-Methoxyphenyl	0.38	74	247-248	4.38
$S_2$3d	4-Chlorophenyl	0.35	77	252-254	4.58
$S_2$3e	4-Nitrophenyl	0.42	80	263-265	4.37
$S_2$4a	Phenyl	0.41	72	237-239	3.72
$S_2$4b	4-Methylphenyl	0.40	72	248-250	4.17
$S_2$4c	4-Methoxyphenyl	0.39	78	257-259	3.93
$S_2$4d	4-Chlorophenyl	0.38	80	258-260	4.30
$S_2$4e	4-Nitrophenyl	0.44	79	269-271	3.72

Solvent system- DCM/methanol (9.5:0.5)
* Log P value was determined using shake flask method.

5.B.1.2. Spectral Characterisation and Elemental Analysis

The structures of compounds were characterised by FT–IR, ^{1}H NMR, ^{13}C downfield signal at δ 182-180 ppm for the carbon linked to sulphur. All other ^{13}C NMR peaks were observed as per the expected chemical shift. The results of the elemental analysis were within ±0.4% of the theoretical values.

1-(2-(3-Oxo-5,6-diphenyl-1,2,4-triazin-2(3*H*)-yl)acetyl)-4 phenylthiosemicarbazide (S₂1a)

Yield: 0.380 g, 76%; mp 202-204°C; R_f 0.44. FT-IR (KBr, cm^{-1}): 3211 and 3113 (N-H); 3005 and 2941 (C-H); 1699 (C=O); 1546 (C=N); 1192 (C=S). ^1H NMR (300 MHz, DMSO-d_6, ppm): δ 10.51 (s, 1H, CONH exchangeable with D_2O); δ 9.86 (s, 1H, CSNH exchangeable with D_2O); δ 8.53 (s, 1H, NH exchangeable with D_2O); δ 7.53-7.13 (m, 15H, Ar–H); δ 3.86 (s, 2H, methylene). ^{13}C NMR (75 MHz, DMSO-d_6, ppm): 180.63, 172.02, 167.04, 165.90, 152.81, 142.66, 139.11, 139.00, 138.91, 138.78, 135.12, 133.84, 131.20, 129.43, 129.16, 128.96, 128.30, 128.17, 125.23, 124.85, 54.77. Anal. calc. for $C_{24}H_{20}N_6O_2S$ C, 63.14; H, 4.42; N, 18.41%; Found: C, 63.37; H, 4.44; N, 18.48%.

1-(2-(3-Oxo-5,6-diphenyl-1,2,4-triazin-2(3*H*)-yl)acetyl)-4-p-tolylthiosemicarbazide (S₂1b)

Yield: 0.365 g, 73%; mp 211-213°C; R_f 0.47. FT-IR (KBr, cm^{-1}): 3109 and 3201 (N-H); 3026 and 2941 (C-H); 1664 (C=O); 1545 (C=N); 1193 (C=S). ^1H NMR (300 MHz, DMSO-d_6, ppm): δ 10.52 (s, 1H, CONH exchangeable with D_2O); δ 9.71 (s, 1H, CSNH exchangeable with D_2O); δ 8.52 (s, 1H, NH exchangeable with D_2O); δ 7.51-7.17 (m, 14H, Ar–H); δ 3.82 (s, 2H, methylene); δ 2.24 (s, 3H, methyl). ^{13}C NMR (75 MHz, DMSO-d_6, ppm): 182.21, 172.12, 167.71, 165.33, 154.09, 142.52, 139.20, 137.42, 134.03, 133.54, 130.48, 130.36, 130.01, 129.11, 128.24, 127.92, NMR (300 MHz, DMSO-d_6, ppm): δ 10.51 (s, 1H, CONH exchangeable with D_2O); δ 9.86 (s, 1H, CSNH exchangeable with D_2O); δ 8.46 (s, 1H, NH exchangeable with D_2O); δ 7.39-7.08 (m, 14H, Ar–H); δ 3.78 (s, 2H, methylene); δ 3.73 (s, 3H, methoxy). ^{13}C NMR (75 MHz, DMSO-d_6, ppm): 180.77, 172.95, 167.05, 165.86, 159.08, 152.81, 142.66, 140.18, 140.04, 135.11, 133.83, 131.19, 129.41, 129.16, 128.95, 128.27, 128.15, 116.68, 55.13, 55.06. Anal. calc. for $C_{25}H_{22}N_6O_3S$: C, 61.71; H, 4.56; N, 17.27%; Found: C, 61.94; H, 4.57; N, 17.32%.

4-(4-Chlorophenyl)-1-(2-(3-oxo-5,6-diphenyl-1,2,4-triazin-2(3*H*)-yl)acetyl) thiosemicarbazide (S$_2$1d)

Yield: 0.415 g, 83%; mp 215-216°C; R$_f$ 0.46. FT-IR (KBr, cm^{-1}): 3238 and 3109 (N-H); 3057 and 2989 (C-H); 1608 (C=O); 1546 (C=N); 1203 (C=S). ^{1}H NMR (300 MHz, DMSO-d_6, ppm): δ 10.51(s, 1H, CONH exchangeable with D_2O); δ 9.96 (s, 1H, CSNH exchangeable with D_2O); δ 8.56 (s, 1H, NH exchangeable with D_2O); δ 7.58-7.29 (m, 14H, Ar–H); δ 3.83 (s, 2H, methylene). ^{13}C NMR (75 MHz, DMSO-d_6, ppm): 181.51, 172.60, 167.00, 165.87, 152.75, 142.61, 138.15, 137.87, 135.09, 133.81, 131.17, 129.41, 129.13, 128.93, 128.27, 128.13, 128.04, 127.95, 126.80, 54.70. Anal. calc. for $C_{24}H_{19}ClN_6O_2S$: C, 58.71; H, 3.90; N, 17.12%; Found: C, 58.69; H, 3.91; N, 17.16%.

4-(4-Nitrophenyl)-1-(2-(3-oxo-5,6-diphenyl-1,2,4-triazin-2(3*H*)-yl)acetyl) thiosemicarbazide (S$_2$1e)

Yield: 0.400 g, 80%; mp 225–226°C; Rf 0.42. FT-IR (KBr, cm^{-1}): 3288 (N-H); 3078 and 2991 (C-H); 1670 (C=O); 1562 (C=N); 1332 (NO); 1205(C=S). ^{1}H NMR (300 MHz, DMSO-d_6, ppm): δ 10.63 (s, 1H, CONH exchangeable with D_2O); δ 9.95

The FT-IR spectra of compounds **($S_2$2a-$S_2$2e)** showed a characteristic absorption peak at 3403-3363 cm^{-1} and 1593-1548 cm^{-1} attributed to N-H and C=N stretching vibration, respectively. The structures were further supported by ^{1}H NMR spectra which showed a multiplet at δ 8.41-6.88 ppm accounting for the aromatic protons. The disappearance of CONH and CSNH singlet signals of thiosemicarbazides (**$S_2$1a-$S_2$1e**) and the retention of NH signal at δ 8.43-8.33 ppm confirmed the formation of 1,3,4-oxadiazole ring. All other ^{13}C NMR peaks were observed as per the expected chemical shift. The results of the elemental analysis were within ±0.4% of the theoretical values.

5,6-Diphenyl-2-((5-(phenylamino)-1,3,4-oxadiazol-2-yl)methyl)-1,2,4-triazin-3(2*H*)-one ($S_2$2a)

FT-IR (KBr, cm^{-1}): 3363 (N-H); 2926 (C-H); 1599 (C=O); 1548 (C=N); 1016 (COC). ^{1}H NMR (300 MHz, DMSO-d_6, ppm): δ 8.33 (s, 1H, NH exchangeable with D_2O); δ 7.57-7.43 (m, 4H, Ar–H); δ 7.41-7.39 (m, 8H, Ar–H); δ 7.31-7.20 (m, 2H, Ar–H); δ 6.93-6.88 (t, 1H, Ar–H); δ 4.21 (s, 2H, methylene). ^{13}C NMR (75 MHz, DMSO-d_6, ppm): 167.19, 165.77, 152.85, 142.85, 142.85, 141.54, 140.41, 139.15, 139.15, 139.15, 135.16, 133.85, 131.12, 129.44, 129.12, 128.22, 126.61, 124.84, 122.10, 117.68, 53.32. Anal. calc. for $C_{24}H_{18}N_6O_2$: C, 68.24; H, 4.29; N, 19.89%; Found: C, 68.50; H, 4.31; N, 19.97%.

2-((5-(p-Tolylamino)-1,3,4-oxadiazol-2-yl)methyl)-5,6-diphenyl-1,2,4-triazin-3(2*H*)-one ($S_2$2b)

FT-IR (KBr, cm^{-1}): 3367 (N-H); 2924 (C-H); 1618 (C=O); 1552 (C=N); 1114 (COC). ^{1}H NMR (300 MHz, DMSO-d_6, ppm): δ 8.36 (s, 1H, NH exchangeable with

2-((5-(4-Methoxyphenylamino)-1,3,4-oxadiazol-2-yl)methyl)-5,6-diphenyl-1,2,4-triazin-3(2*H*)-one (S₂2c)

FT-IR (KBr, cm^{-1}): 3372 (N-H); 2933, 2835 (C-H); 1606 (C=O); 1558 (C=N); 1030 (COC). ^{1}H NMR (300 MHz, DMSO-d_6, ppm): δ 8.36 (s, 1H, NH exchangeable with D_2O); δ 7.63-7.06 (m, 14H, Ar–H); δ 4.33 (s, 2H, methylene); δ 3.69 (s, 3H, methoxy). ^{13}C NMR (75 MHz, DMSO-d_6, ppm): 167.83, 165.00, 156.22, 147.90, 142.32, 136.02, 133.65, 131.04, 130.66, 130.52, 130.25, 130.16, 129.83, 129.51, 129.19, 128.06, 127.90, 126.29, 125.96, 122.88, 119.58, 55.32, 54.29. Anal. calc. for $C_{25}H_{20}N_6O_3$: C, 66.36; H, 4.46; N, 18.57%; Found: C, 66.60; H, 4.48; N, 18.64%.

2-((5-(4-Chlorophenylamino)-1,3,4-oxadiazol-2-yl)methyl)-5,6-diphenyl-1,2,4-triazin-3(2*H*)-one (S₂2d)

FT-IR (KBr, cm^{-1}): 3403 (N-H); 2928 (C-H); 1614 (C=O); 1554 (C=N); 1091 (COC). ^{1}H NMR (300 MHz, DMSO-d_6, ppm): δ 8.43 (s, 1H, NH exchangeable with D_2O); δ 7.70-6.98 (m, 14H, Ar–H); δ 4.25 (s, 2H, methylene). ^{13}C NMR (75 MHz, DMSO-d_6, ppm): 167.22, 165.63, 152.15, 142.90, 139.83, 139.29, 138.63, 135.16, 133.85, 131.13, 129.46, 129.18, 128.97, 128.90, 128.79, 128.24, 128.08, 125.43, 124.62, 118.97, 54.16. Anal. calc. for $C_{24}H_{17}ClN_6O_2$: C, 63.09; H, 3.75; N, 18.39%; Found: C, 63.33; H, 3.76; N, 18.46%.

2-((5-(4-Nitrophenylamino)-1,3,4-oxadiazol-2-yl)methyl)-5,6-diphenyl-1,2,4-triazin-3(2*H*)-one (S₂2e)

FT-IR (KBr, cm^{-1}): 3365 (N-H); 3086 and 2926 (C-H); 1627 (C=O); 1593 (C=N), 1332 (NO); 1111 (COC). ^{1}H NMR (300 MHz, DMSO-d_6, ppm): δ 8.42 (s, 1H, NH

The FT-IR spectrum of compounds **($S_2$3a-$S_2$3e)** showed an absorption peak at 1599-1527 cm^{-1} marking the presence of C=N stretching vibrations. Singlet corresponding to CONH and CSNH protons were absent in the ^{1}H NMR spectrum, and a multiplet confirming the existence of aromatic protons was observed in region δ 8.40-6.94 ppm. Apart from this, the NH protons were found as a singlet at δ 8.42-8.36 ppm which established the structure of the compounds. All other ^{13}C NMR peaks were observed as per the expected chemical shift. The results of the elemental analysis were within ±0.4% of the theoretical values.

5,6-Diphenyl-2-((5-(phenylamino)-1,3,4-thiadiazol-2-yl)methyl)-1,2,4-triazin-3(2*H*)-one ($S_2$3a)

FT-IR (KBr, cm^{-1}): 3205 (N-H); 2939 (C-H); 1658 (C=O); 1599 (C=N). ^{1}H NMR (300 MHz, DMSO-d_6, ppm): δ 8.37 (s, 1H, NH exchangeable with D_2O); δ 7.52-6.95 (m, 15H, Ar–H); δ 4.28 (s, 2H, methylene). ^{13}C NMR (75 MHz, DMSO-d_6, ppm): 167.29, 165.97, 153.75, 142.72, 141.44, 140.30, 139.13, 135.12, 133.83, 131.11, 129.30, 129.11, 128.21, 126.60, 124.83, 122.10, 117.68, 54.02. Anal. calc. for $C_{24}H_{18}N_6OS$: C, 65.74; H, 4.14; N, 19.17%; Found: C, 65.98; H, 4.15; N, 19.24%.

2-((5-(p-Tolylamino)-1,3,4-thiadiazol-2-yl)methyl)-5,6-diphenyl-1,2,4-triazin-3(2*H*)-one ($S_2$3b)

FT-IR (KBr, cm^{-1}): 3309 (N-H); 2928 (C-H); 1558 (C=O); 1527 (C=N). ^{1}H NMR (300 MHz, DMSO-d_6, ppm): δ 8.41 (s, 1H, NH exchangeable with D_2O); δ 7.83-7.80 (d, 1H, Ar–H); δ 7.65-7.63 (d, 1H, Ar–H); δ 7.26-7.15 (m, 10H, Ar–H); δ 7.02-6.94 (m, 2H, Ar–H); δ 4.32 (s, 2H, methylene); δ 2.25 (s, 3H, methyl). ^{13}C

2-((5-(4-Methoxyphenylamino)-1,3,4-thiadiazol-2-yl)methyl)-5,6-diphenyl-1,2,4-triazin-3(2*H*)-one (S₂3c)

FT-IR (KBr, cm^{-1}): 3381 (N-H); 2902 (C-H); 1664 (C=O); 1585 (C=N). ^{1}H NMR (300 MHz, DMSO-d_6, ppm): δ 8.36 (s, 1H, NH exchangeable with D_2O); δ 7.69-7.26 (m, 14H, Ar–H); δ 4.29 (s, 2H, methylene); δ 3.72 (s, 3H, methoxy). ^{13}C NMR (75 MHz, DMSO-d_6, ppm): 168.62, 165.60, 156.92, 148.22, 142.60, 136.44, 133.91, 131.40, 130.96, 130.86, 130.56, 130.46, 130.00, 129.80, 129.50, 128.39, 128.13, 126.50, 126.11, 123.05, 119.80, 55.26, 54.50. Anal. calc. for $C_{25}H_{20}N_6O_2S$: C, 64.09; H, 4.30; N, 17.94%; Found: C, 64.33; H, 4.28; N, 17.99%.

2-((5-(4-Chlorophenylamino)-1,3,4-thiadiazol-2-yl)methyl)-5,6-diphenyl-1,2,4-triazin-3(2*H*)-one (S₂3d)

FT-IR (KBr, cm^{-1}): 3257 (N-H); 3055 (C-H); 1658 (C=O); 1599 (C=N). ^{1}H NMR (300 MHz, DMSO-d_6, ppm): δ 8.40 (s, 1H, NH exchangeable with D_2O); δ 8.21-7.28 (m, 14H, Ar–H); δ 4.27 (s, 2H, methylene). ^{13}C NMR (75 MHz, DMSO-d_6, ppm): 167.23, 165.68, 152.15, 142.89, 139.83, 139.29, 138.63, 135.17, 133.85, 131.13, 129.47, 129.18, 128.98, 128.90, 128.78, 128.24, 128.07, 125.43, 124.62, 118.98, 54.36. Anal. calc. for $C_{24}H_{17}ClN_6OS$: C, 60.95; H, 3.62; N, 17.77%; Found: C, 61.18; H, 3.63; N, 17.70%.

2-((5-(4-Nitrophenylamino)-1,3,4-thiadiazol-2-yl)methyl)-5,6-diphenyl-1,2,4-triazin-3(2*H*)-one (S₂3e)

FT-IR (KBr, cm^{-1}): 3259 (N-H); 3059 (C-H); 1651 (C=O); 1597 (C=N); 1330 (NO). ^{1}H NMR (300 MHz, DMSO-d_6, ppm): δ 8.42 (s, 1H, NH exchangeable with

The formation of the 1,2,4-triazole ring in compounds (**$S_2$4a-$S_2$4e**) was supported by its ^{1}H NMR spectrum which showed a singlet corresponding to SH proton at δ 11.31-11.26 ppm in addition to the aromatic protons at δ 8.20-6.46 ppm. All other ^{13}C NMR peaks were observed as per the expected chemical shift. The results of the elemental analysis were within ±0.4% of the theoretical values.

2-((5-Mercapto-4-phenyl-4H-1,2,4-triazol-3-yl)methyl)-5,6-diphenyl-1,2,4-triazin-3(2*H*)-one (S$_2$4a)

FT-IR (KBr, cm^{-1}): 2928 (C-H); 1597 (C=O); 1543 (C=N). ^{1}H NMR (500 MHz, DMSO-d_6, ppm): δ 11.27 (s, 1H, SH exchangeable with D_2O); δ 7.53-7.17 (m, 15H, Ar–H); δ 4.25 (s, 2H, methylene). ^{13}C NMR (125 MHz, DMSO-d_6, ppm): 167.27, 165.27, 159.18, 148.68, 142.47, 141.39, 134.17, 133.21, 131.12, 130.81, 130.72, 130.37, 130.17, 129.94, 129.84, 129.47, 129.17, 129.03, 128.72, 125.84, 121.91, 118.31, 54.23. Anal. calc. for $C_{24}H_{18}N_6OS$: C, 65.74; H, 4.14; N, 19.17%; Found: C, 65.89; H, 4.15; N, 19.20%.

2-((5-Mercapto-4-p-tolyl-4H-1,2,4-triazol-3-yl)methyl)-5,6-diphenyl-1,2,4-triazin-3(2*H*)-one (S$_2$4b)

FT-IR (KBr, cm^{-1}): 2926 (C-H); 1618 (C=O); 1593 (C=N). ^{1}H NMR (300 MHz, DMSO-d_6, ppm): δ 11.27 (s, 1H, SH exchangeable with D_2O); δ 7.47-6.98(m, 14H, Ar–H); δ 4.26 (s, 2H, methylene); δ 2.24 (s, 3H, methyl). ^{13}C NMR (75 MHz, DMSO-d_6, ppm): 168.62, 165.03, 159.67, 149.57, 137.73, 136.79, 131.63, 131.03, 130.95, 130.42, 130.36, 129.92, 129.43, 127.43, 127.07, 126.41, 126.24, 124.30, 123.16, 122.45, 119.63, 53.68, 25.24. Anal. calc. for $C_{25}H_{20}N_6OS$: C, 66.35; H, 4.45; N, 18.57%; Found: C, 66.48; H, 4.46; N, 18.61%.

DMSO-d_6, ppm): 168.55, 165.21, 162.61, 159.61, 148.03, 141.23, 137.86, 136.04, 133.55, 130.16, 129.35, 129.21, 128.68, 128.50, 125.11, 122.30, 121.18, 116.91, 55.39, 54.92. Anal. calc. for $C_{25}H_{20}N_6O_2S$: C, 64.09; H, 4.30; N, 17.94%; Found: C, 63.92; H, 4.29; N, 17.89%.

2-((4-(4-Chlorophenyl)-5-mercapto-4H-1,2,4-triazol-3-yl)methyl)-5,6-diphenyl-1,2,4-triazin-3(2*H*)-one (S24d)

FT-IR (KBr, cm^{-1}): 2928 (C-H); 1703 (C=O); 1546 (C=N). ^{1}H NMR (500 MHz, DMSO-d_6, ppm): δ 11.26 (s, 1H, SH exchangeable with D_2O); δ 7.91-7.22 (m, 14H, Ar–H); δ 4.28 (s, 2H, methylene). ^{13}C NMR (125 MHz, DMSO-d_6, ppm): 168.93, 165.73, 159.26, 148.40, 141.75, 139.42, 134.84, 133.37, 131.99, 131.63, 131.33, 130.68, 130.34, 129.61, 129.08, 128.17, 127.69, 125.54, 119.89, 54.27. Anal. calc. for $C_{24}H_{17}ClN_6OS$: C, 60.95; H, 3.62; N, 17.77%; Found: C, 60.83; H, 3.61; N, 17.73%.

2-((5-Mercapto-4-(4-nitrophenyl)-4H-1,2,4-triazol-3-yl)methyl)-5,6-diphenyl-1,2,4-triazin-3(2*H*)-one (S24e)

FT-IR (KBr, cm^{-1}): 3099 (C-H); 1593 (C=O); 1506 (C=N); 1330 (NO). ^{1}H NMR (500 MHz, DMSO-d_6, ppm): δ 11.31 (s, 1H, SH exchangeable with D_2O); δ 8.20-8.14 (d, 2H, Ar–H); δ 7.76-7.46 (d, 2H, Ar–H); δ 7.54-7.13 (m, 10H, Ar–H); δ 4.28 (s, 2H, methylene). ^{13}C NMR (125 MHz, DMSO-d_6, ppm): 169.09, 166.13, 159.45, 148.57, 141.21, 139.70, 134.07, 133.03, 131.47, 131.13, 130.93, 130.25, 129.87, 129.39, 129.11, 128.96, 128.66, 128.32, 128.14, 127.95, 127.59, 125.24, 119.46, 54.57. Anal. calc. for $C_{24}H_{17}N_7O_3S$: C, 59.62; H, 3.54; N, 20.28%; Found: C, 59.73; H, 3.55; N, 20.31%.

5.B.2. BIOLOGICAL ACTIVITY

5.B.2.1. Evaluation of Anti-Inflammatory Activity

5.B.2.1.1. Albumin Denaturation Assay

The albumin denaturation assay was performed to observe the preliminary anti-inflammatory potential of the synthesised compounds. The result of the initial screening of all the synthesised compounds by albumin denaturation assay is presented in **Table 5.14**. Protein stabilisation by the compounds **(S$_2$2a-S$_2$2e, S$_2$3a-S$_2$3e, S$_2$4a-S$_2$4e)** was indicated by the test compounds and standard drugs (indomethacin and celecoxib) compared to the control.

TABLE 5.14. Albumin Denaturation Assay

Comp.	Absorbance	% Inhibition	Comp.	Absorbance	% Inhibition
Control	0.1258 ± 0.0079	--	**S$_2$3b**	0.2102 ± 0.0184^a	67.10
Indo 10	0.2298 ± 0.0184^a	82.67	**S$_2$3c**	0.2235 ± 0.0132^a	77.66
Celecoxib	0.2268 ± 0.0166^a	80.29	**S$_2$3d**	0.2228 ± 0.0108^a	77.11
S$_2$2a	0.2046 ± 0.0125^a	62.64	**S$_2$3e**	0.2237 ± 0.0204^a	77.82
S$_2$2b	0.2049 ± 0.0110^a	62.88	**S$_2$4a**	0.1896 ± 0.0162	50.71
S$_2$2c	0.2240 ± 0.0148^a	78.06	**S$_2$4b**	0.1913 ± 0.0128	52.07
S$_2$2d	0.2249 ± 0.0173^a	78.77	**S$_2$4c**	0.1952 ± 0.0117	55.17
S$_2$2e	0.2255 ± 0.0109^a	79.25	**S$_2$4d**	0.2163 ± 0.0202^a	71.94
S$_2$3a	0.2040 ± 0.0146^a	62.16	**S$_2$4e**	0.2165 ± 0.0180^a	72.10

Values are expressed as the Mean ± S.D (n = 3); **a**: $p < 0.05$ vs. Control; **Indo 10:** Indomethacin 10 mg; **Celecoxib** and other test compounds were administered in 0.3% w/v sodium CMC at an equimolar oral dose relative to 10 mg indomethacin.

Hybrids **S$_2$2c-S$_2$2e, S$_2$3c-S$_2$3e, S$_2$4d** and **S$_2$4e** exhibited inhibition (71.94-79.25%) as compared to the standard drugs indomethacin (82.67%) and celecoxib (80.29%). Compounds failing to elicit a minimum of 70% inhibition of evaluated compounds were well tolerated up to a dose of 500 mg/kg. Also, no mortality was observed up to 14 days post administration, even at the highest dose of 500 mg/kg body weight, which suggested an appreciable margin of safety.

5.B.2.1.3. Carrageenan-Induced Rat Paw Oedema

The selected compounds **(S$_2$2c-S$_2$2e**, **S$_2$3c-S$_2$3e**, **S$_2$4d** and **S$_2$4e**,**)** were evaluated for carrageenan-induced rat paw oedema anti-inflammatory activity. The outcome of the anti-inflammatory effects of the compounds **S$_2$2c-S$_2$2e**, **S$_2$3c-S$_2$3e**, **S$_2$4d** and **S$_2$4e** is summarised in **Table 5.15**. With the exception of hybrids **S$_2$4d** and **S$_2$4e,** all the evaluated compounds exhibited marked inhibition of the oedema in comparison to the standard drugs indomethacin and celecoxib. The maximum percentage inhibition was observed at 5 h and discussed accordingly.

From the results presented in **Table 5.15**, it is apparent that compounds **S$_2$2d** and **S$_2$2e** possessed a fast onset of action (post 2 h) as compared to others. Amongst the evaluated compounds, six were found to exhibit anti-inflammatory activity (57.90-61.56% reduction in inflammation). Compound **S$_2$2e** bearing an electron withdrawing 4-nitrophenyl group on the five-member 1,3,4-oxadiazole ring elicited excellent protection against inflammation (61.56%) comparable to standard drugs indomethacin (63.56%) and celecoxib (62.26%), respectively. It was followed by **S$_2$2d** and **S$_2$2c**, also bearing electron withdrawing groups 4-chlorophenyl and 4-methoxyphenyl at the fifth position of the 1,3,4-oxadiazole ring showing the inhibition of 60.97% and 60.85% respectively.

Compounds **S$_2$3c**-**S$_2$3e** bearing a bioisosteric replacement of the 1,3,4-oxadiazole with a 1,3,4-thiadiazole ring bearing an electron withdrawing

TABLE 5.15. Carrageenan-Induced Paw Oedema

Compound	**Swelling thickness in mm (% Inhibition)**						
	0 h	**1 h**	**2 h**	**3 h**	**4 h**	**5 h**	**6 h**
Control	3.23 ± 0.26	8.02 ± 0.63	8.68 ± 0.67	8.80 ± 0.64	8.72 ± 0.68	8.48 ± 0.63	8.23 ± 0.68
Indo 10	3.02 ± 0.21	3.59 ± 0.23[a] (55.24)	3.60 ± 0.27[a] (58.52)	3.30 ± 0.22[a] (62.50)	3.21 ± 0.25[a] (63.19)	3.09 ± 0.28[a] (63.56)	3.26 ± 0.19[a] (60.39)
Celecoxib	3.12 ± 0.20	3.75 ± 0.30[a] (53.24)	3.81 ± 0.35[a] (56.11)	3.35 ± 0.31[a] (61.93)	3.23 ± 0.29[a] (62.96)	3.20 ± 0.22[a] (62.26)	3.19 ± 0.30[a] (61.24)
$S_2$2c	3.19 ± 0.29	5.04 ± 0.45[abc] (37.16)	4.84 ± 0.44[abc] (44.24)	3.93 ± 0.36[ab] (55.34)	3.51 ± 0.32[a] (59.75)	3.32 ± 0.25[a] (60.85)	3.29 ± 0.29[a] (60.02)
$S_2$2d	3.07 ± 0.23	4.91 ± 0.45[abc] (38.78)	4.68 ± 0.41[abc] (46.08)	3.74 ± 0.32[a] (57.50)	3.53 ± 0.29[a] (59.52)	3.31 ± 0.23[a] (60.97)	3.28 ± 0.31[a] (60.14)
$S_2$2e	3.19 ± 0.27	4.95 ± 0.42[abc] (38.28)	4.76 ± 0.44[abc] (45.16)	3.58 ± 0.31[a] (59.32)	3.45 ± 0.29[a] (60.43)	3.26 ± 0.28[a] (61.56)	3.26 ± 0.24[a] (60.39)
$S_2$3c	3.24 ± 0.20	5.20 ± 0.50[abc] (35.16)	4.97 ± 0.47[abc] (42.74)	3.94 ± 0.35[ab] (55.23)	3.56 ± 0.31[a] (59.17)	3.46 ± 0.20[a] (59.20)	3.43 ± 0.33[a] (58.32)
$S_2$3d	3.31 ± 0.28	5.31 ± 0.46[abc] (33.79)	5.20 ± 0.48[abc] (40.10)	4.07 ± 0.36[abc] (53.75)	3.75 ± 0.34[a] (56.99)	3.57 ± 0.31[a] (57.90)	3.59 ± 0.33[a] (56.38)
$S_2$3e	3.15 ± 0.22	5.07 ± 0.43[abc] (36.78)	4.79 ± 0.37[abc] (44.81)	3.92 ± 0.33[ab] (55.45)	3.63 ± 0.31[a] (58.37)	3.52 ± 0.30[a] (58.49)	3.36 ± 0.32[a] (59.17)
$S_2$4d	3.28 ± 0.22	5.74 ± 0.52[abc] (28.43)	6.05 ± 0.58[abc] (30.30)	5.38 ± 0.44[abc] (38.86)	4.98 ± 0.36[abc] (42.89)	4.80 ± 0.39[abc] (43.40)	4.71 ± 0.45[abc] (42.77)
$S_2$4e	3.45 ± 0.28	6.01 ± 0.41[abc] (25.06)	6.18 ± 0.40[abc] (28.80)	6.18 ± 0.55[abc] (29.77)	5.82 ± 0.52[abc] (33.26)	5.25 ± 0.49[abc] (38.09)	5.29 ± 0.43[abc] (35.72)

Values are expressed as the Mean ± S.D (n = 6).; **a**: $p < 0.05$ vs. Control; **b**: $p < 0.05$ vs. Indo; **c**: $p < 0.05$ vs. Celecoxib; **Control:** 0.3% w/v sodium in distilled water (10 ml/kg, *p.o.*); **Indo 10:** Indomethacin (10 mg/kg, *p.o*) in 0.3% w/v sodium CMC; **Celecoxib** and other test compounds were administered in 0.3% w/v sodium CMC at an equimolar oral dose relative to 10 mg/kg indomethacin.

5.B.2.1.4. Arachidonic Acid-Induced Rat Paw Oedema

The selected compounds **($S_2$2c-$S_2$2e** and **$S_2$3c-$S_2$3e)** were subjected to anti-inflammatory activity against arachidonic acid induced rat paw oedema to distinguish COX and LOX inhibition (Di Martino *et al.*, 1987). The result of the arachidonic acid induced rat paw oedema bioassay is presented in **Table 5.16**. A sub-plantar injection of arachidonic acid produced significant oedema as after 30 min and reached a maximum at 60 min.

TABLE 5.16. Arachidonic Acid Induced Paw Oedema

Compound	**Swelling thickness (mm)**	
	1 h	**% Inhibition**
Control	5.84 ± 0.37	–
ZIL 10	1.76 ± 0.08^{a}	69.86
Indo 10	4.48 ± 0.32^{ab}	23.29
Celecoxib	4.34 ± 0.35^{ab}	25.68
$S_2$2c	4.66 ± 0.33^{ab}	20.20
$S_2$2d	4.60 ± 0.37^{ab}	21.23
$S_2$2e	4.58 ± 0.32^{ab}	21.57
$S_2$3c	4.63 ± 0.35^{ab}	20.72
$S_2$3d	4.69 ± 0.36^{ab}	19.69
$S_2$3e	4.72 ± 0.38^{ab}	19.18

Values are expressed as the Mean ± S.D (n = 6); **a**: $p < 0.05$ vs. Control; **b**: $p < 0.05$ vs. Zileuton; **Control:** 0.3% w/v sodium CMC in distilled water (10 ml/kg, *p.o.*); **ZIL 10:** Zileuton (10 mg/kg, *p.o*) in 0.3% w/v sodium CMC; **Indo 10:** Indomethacin (10 mg/kg, *p.o*) in 0.3% w/v sodium CMC; **Celecoxib** and other test compounds were administered in 0.3% w/v sodium CMC at an equimolar oral dose relative to 10 mg/kg indomethacin.

Oral administration of the compounds **$S_2$2c-$S_2$2e** and **$S_2$3c-$S_2$3e** failed to

5.B.2.1.5. Cotton Pellet-Induced Granuloma in Rats

The selected compounds were evaluated for subchronic anti-inflammatory activity using cotton pellet induced granuloma method which has been extensively employed to assess the transudative, exudative and proliferative components of subchronic inflammation (Spector, 1969). The fluid adsorbed by the pellet significantly influences the wet weight of the granuloma, whereas the dry weight correlates well with the amount of granulomatous tissue formed (Panthong *et al.*, 2003). The effect of the derivatives (**$S_2$2c-$S_2$2e, $S_2$3c-$S_2$3e)** along with standard indomethacin and celecoxib on cotton pellet induced granuloma in rats is presented in **Table 5.17**.

TABLE 5.17. Cotton Pellet Induced Granuloma

Compound	Wt. of granulation (mg)
Control	90.72 ± 6.28
Indo 10	51.68 ± 3.83^a
Celecoxib	53.24 ± 3.38^a
$S_2$2c	54.78 ± 4.04^a
$S_2$2d	54.19 ± 3.67^a
$S_2$2e	55.24 ± 4.05^a
$S_2$3c	55.82 ± 3.92^a
$S_2$3d	55.82 ± 4.17^a
$S_2$3e	55.93 ± 4.11^a

Values are expressed as the Mean ± S.D (n = 6); **a**: $p < 0.05$ vs. Control; **Control:** 0.3% w/v sodium CMC in distilled water (10 ml/kg, *p.o.*); **Indo 10:** Indomethacin (10 mg/kg, *p.o*) in 0.3% w/v sodium CMC; **Celecoxib** and other test compounds were administered in 0.3% w/v sodium CMC at an equimolar oral dose relative to 10 mg/kg indomethacin.

In this study, the compounds **$S_2$2c-$S_2$2e, $S_2$3c-$S_2$3e** and the standard drugs decreased both the wet and dry weight of the cotton pellets as compared to the rheumatoid arthritis is a chronic destructive inflammatory polyarticular disease of the joints which is characterised by massive synovial proliferation and systemic and local inflammation causing cartilage and bone destruction. In the investigation of Freund's complete adjuvant (FCA) induced arthritis, it was observed that the paw swelling and thickness which developed over a period of 24 h post adjuvant injection, subsided slightly for next 5-8 days and then increased when arthritis appeared. The treatment which was initiated 14 days post adjuvant induction suppressed the subsequent increase in swelling of the injected foot, which occurred, with the appearance of polyarthritis. The determination of foot thickness of the rats was used in evaluating anti-inflammatory activity and therapeutic effects of the treatment. The result of the Freund's adjuvant induced arthritis in rats is depicted in **Table 5.18**.

It was observed that the compounds **$S_2$2c-$S_2$2e**, **$S_2$3c-$S_2$3e** and the standard drugs exhibited anti-arthritic effect evidenced by a significant progressive reduction in paw swelling compared with arthritic control animals ($p < 0.05$) for 21 days. It is evident from the reported literature that FCA induces arthritis, where both T cell and B cell activation play a significant role. Cytokines of Th1 (IFNγ secreting) and Th2 cells (IL-4 secreting) are generated wherein Th1 profile predominates at the onset of disease (Courtenay *et al.*, 1980). Thus, the ability of the compounds to reduce oedema formation may be imputed to their inhibitory effects on cytokines in addition to prostaglandins.

5.B.2.1.7. Evaluation of Ulcerogenic Liability & Lipid Peroxidation Studies

Compounds exhibiting prominent *in-vivo* anti-inflammatory profiles were further evaluated for their ulcerogenic liability. The results depicted in **Table**

TABLE 5.18. Adjuvant-Induced Arthritis, Ulcer Index and Lipid Peroxidation

Compound	Paw thickness (mm)							Ulcer Index ± S.D	nmol for MDA content ± S.D 100 mg^{-1} tissue
	Day 03	Day 06	Day 09	Day 12	Day 15	Day 18	Day 21		
Control	7.92 ± 0.58	8.10 ± 0.62	8.32 ± 0.60	8.38 ± 0.64	8.44 ± 0.60	8.51 ± 0.63	8.56 ± 0.61	0	4.24 ± 0.34
Indo 10	5.53 ± 0.40^{a} (30.18)	4.96 ± 0.42^{a} (38.77)	4.62 ± 0.42^{a} (44.47)	4.47 ± 0.41^{a} (46.66)	3.96 ± 0.35^{a} (53.08)	3.54 ± 0.33^{a} (58.40)	3.45 ± 0.31^{a} (59.70)	55 ± 3.8	8.38 ± 0.57^{a}
Celecoxib	5.44 ± 0.46^{a} (31.31)	5.11 ± 0.43^{a} (36.91)	4.96 ± 0.34^{a} (40.38)	4.76 ± 0.41^{a} (43.20)	4.25 ± 0.40^{a} (49.64)	3.99 ± 0.35^{a} (53.11)	3.77± 0.32^{a} (55.96)	26 ± 1.9	6.82 ± 0.54^{ab}
S$_2$2c	5.67 ± 0.47^{a} (28.41)	5.53 ± 0.52^{ab} (31.73)	5.09 ± 0.44^{a} (38.82)	4.90 ± 0.42^{a} (41.53)	4.57 ± 0.43^{a} (45.85)	4.41 ± 0.40^{ab} (48.18)	4.14 ± 0.38^{a} (51.64)	22 ± 1.8	4.67 ± 0.35^{abc}
S$_2$2d	5.77 ± 0.55^{a} (27.15)	5.64 ± 0.43^{a} (30.37)	5.23 ± 0.46^{a} (37.14)	4.94 ± 0.41^{a} (41.05)	4.48 ± 0.37^{a} (46.92)	4.33 ± 0.41^{ab} (49.12)	4.09 ± 0.36^{a} (52.22)	20 ± 1.1	4.18 ± 0.37^{abc}
S$_2$2e	5.52 ± 0.42^{a} (30.30)	5.35 ± 0.47^{a} (33.95)	5.05 ± 0.45^{a} (39.30)	4.68 ± 0.41^{a} (44.15)	4.28 ± 0.39^{a} (49.29)	3.96 ± 0.36^{a} (53.47)	3.83 ± 0.35^{a} (55.26)	24 ± 2.0	4.31 ± 0.39^{abc}
S$_2$3c	5.74 ± 0.48^{a} (27.53)	5.66 ± 0.43^{ab} (30.12)	5.40 ± 0.31^{ab} (35.10)	4.85 ± 0.43^{a} (42.12)	4.70 ± 0.40^{ab} (44.31)	4.39 ± 0.38^{ab} (48.41)	4.12 ± 0.28^{a} (51.87)	23 ± 1.5	4.54 ± 0.38^{abc}
S$_2$3d	5.57 ± 0.51^{a} (29.67)	5.44 ± 0.41^{a} (32.84)	5.35 ± 0.43^{ab} (35.70)	5.11 ± 0.45^{a} (39.02)	4.83 ± 0.47^{ab} (42.77)	4.45 ± 0.42^{ab} (47.71)	4.20 ± 0.37^{ab} (50.93)	24 ± 2.2	4.83 ± 0.33^{abc}
S$_2$3e	5.68 ± 0.54^{a} (28.28)	5.62 ± 0.48^{a} (30.62)	5.30 ± 0.50^{a} (36.30)	4.90 ± 0.30^{a} (41.53)	4.72 ± 0.42^{ab} (44.08)	4.47 ± 0.41^{ab} (47.47)	4.18 ± 0.28^{ab} (51.17)	22 ± 1.3	5.02 ± 0.41^{abc}

Values are expressed as the Mean ± S.D (n = 6); **a**: $p < 0.05$ vs. Control; **b**: $p < 0.05$ vs. Indo 10; **c**: $p < 0.05$ vs. Celecoxib; **Control:** 0.3% w/v sodium CMC in distilled water (10 ml/kg, *p.o.*); **Indo 10:** Indomethacin (10 mg/kg, *p.o*) in 0.3% w/v sodium CMC; **Celecoxib** and other test compounds were administered in 0.3% w/v sodium CMC at an equimolar oral dose relative to 10 mg/kg indomethacin.

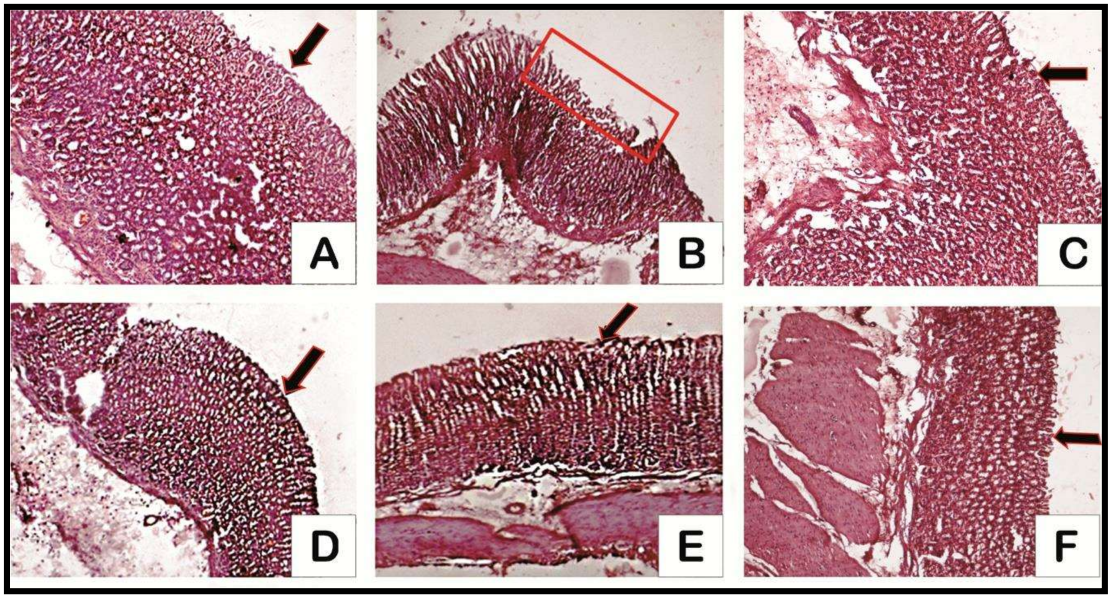

Figure 5.10. Photomicrographs (10x magnification) of **[A]** Control group; **[B]**: Indomethacin; **[C]**: Celecoxib; **[D]**: Compound **S$_2$2d** **[E]**: Compound **S$_2$2e** **[F]**: Compound **S$_2$3c** treated groups in rat stomach tissues (hematoxylin and eosin staining). [Indications: Red box indicates severe detachment of surface epithelium, resulting in the formation of gastric lesions, Arrows indicates the typical stomach architecture with little or no ulcer formation]**.**

Further, the lipid peroxidation profile (**Table 5.18**) of the compounds **S$_2$2c-S$_2$2e** and **S$_2$3c-S$_2$3e** was assessed to validate the results of ulcerogenic activity since compounds eliciting less ulcerogenic liability also exhibited reduced MDA content, a by-product of lipid peroxidation (Pohle *et al.*, 2001). Apart from eliciting minimal ulcerogenic liability, the compounds also exhibited a marked reduction in lipid peroxidation. Indomethacin elicited the highest lipid peroxidation, 8.38±0.57 nmol MDA 100 mg^{-1} tissue, whereas the control group exhibited a lipid peroxidation of 4.24±0.34 nmol MDA 100 mg^{-1} tissue under similar experimental conditions. These results further support the protective effect of the compounds on the inhibition of lipid peroxidation in the gastric

Table 5.19. The results confirmed their relative hepatic and renal safety compared with the standard drugs for prolonged use. This was further established by the histological studies of both the organs (**Fig. 5.11** and **Fig. 5.12**), which exhibited very little or no inflammatory cell infiltrate, oedema, epithelial cell loss, necrosis or degeneration in hepatocytes and nephrons, respectively, compared to the indomethacin-treated group.

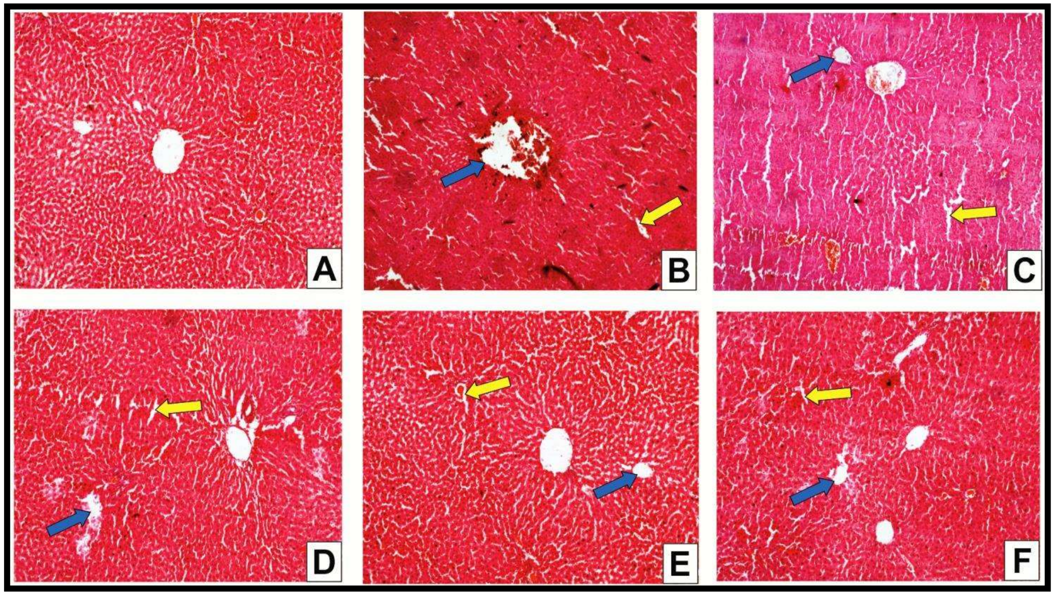

Figure 5.11. Photomicrographs (10x magnification) of **[A]** Control; **[B]** Indomethacin; **[C]** Celecoxib **[D]** Compound **$S_2$2d** **[E]**: Compound **$S_2$2e** **[F]**: Compound **$S_2$3c** treated groups in rat liver tissues (hematoxylin and eosin staining). Blue arrows indicate fibrosis and fatty degeneration. Yellow arrows indicate dilated sinusoids.

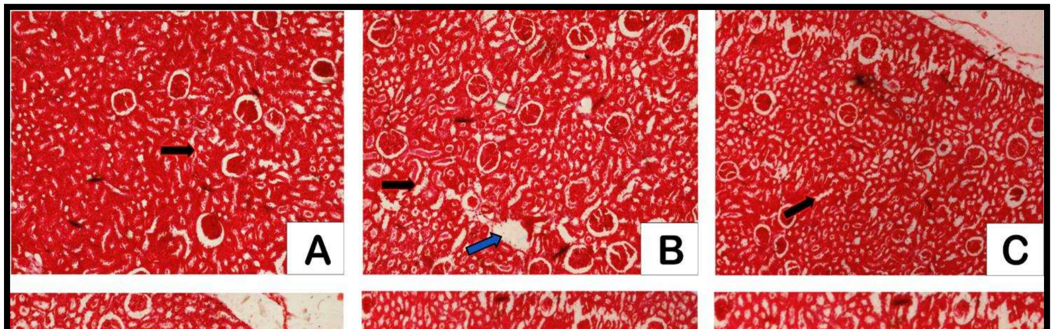

TABLE 5.19. Effect of Selected Potential Compounds on Hepatic and Renal Toxicity Parameters as Evaluated on 21st Day after Treatment

Compound	SGOT (U/mL)	SGPT (U/mL)	ALP (U/mL)	Total protein (g/dL)	Total albumin (g/dL)	CR (mg/dL)	BUN (mg/dL)
Control	90.87 ± 6.38	31.36 ± 2.20	18.12 ± 0.96	1.91 ± 0.13	1.62 ± 0.09	0.58 ± 0.039	21.88 ± 1.42
Indo 10	118.68 ± 8.23^{a}	51.34 ± 3.91^{a}	27.18 ± 1.53^{a}	2.32 ± 0.15^{a}	2.48 ± 0.17^{a}	1.91 ± 0.12^{a}	63.17 ± 1.54^{a}
Celecoxib	113.56 ± 8.38^{a}	48.33 ± 3.65^{a}	25.83 ± 1.68^{a}	2.21 ± 0.15^{a}	2.30 ± 0.14^{a}	1.32 ± 0.07^{ab}	61.38 ± 1.49^{a}
$S_2$2c	97.89 ± 7.68^{bc}	38.11 ± 3.09^{abc}	20.67 ± 1.23^{bc}	2.02 ± 0.14^{b}	1.82 ± 0.14^{bc}	0.91 ± 0.05^{abc}	42.78 ± 1.32^{abc}
$S_2$2d	98.77 ± 7.42^{bc}	41.34 ± 3.15^{abc}	21.34 ± 1.55^{abc}	2.03 ± 0.17^{b}	1.92 ± 0.15^{abc}	1.17 ± 0.07^{abc}	45.78 ± 1.36^{abc}
$S_2$2e	98.12 ± 7.18^{bc}	38.88 ± 2.94^{abc}	20.97 ± 1.56^{abc}	1.98 ± 0.13^{b}	1.88 ± 0.16^{bc}	1.04 ± 0.07^{abc}	45.17 ± 1.36^{abc}
$S_2$3c	96.91 ± 6.98^{bc}	40.20 ± 3.34^{abc}	21.09 ± 1.62^{abc}	2.00 ± 0.12^{b}	1.96 ± 0.17^{abc}	0.95 ± 0.06^{abc}	47.24 ± 1.34^{abc}
$S_2$3d	97.23 ± 7.07^{bc}	39.78 ± 3.11^{abc}	22.11 ± 1.66^{abc}	1.97 ± 0.16^{b}	1.87 ± 0.18^{bc}	1.08 ± 0.05^{abc}	48.71 ± 1.41^{abc}
$S_2$3e	97.88 ± 7.41^{bc}	41.97 ± 3.57^{abc}	22.54 ± 1.60^{abc}	2.00 ± 0.18^{b}	1.95 ± 0.17^{abc}	1.20 ± 0.08^{abc}	49.83 ± 1.40^{abc}

SGOT: Serum Glutamic Oxaloacetic Transaminase; **SGPT:** Serum Glutamic Pyruvic Transaminase; **ALP:** Alkaline Phosphatase; **CR:** Creatinine; **BUN:** Blood Urea Nitrogen; Values are expressed as the Mean ± S.D (n = 6); **a**: $p < 0.05$ vs. Control; **b**: $p < 0.05$ vs. Indo 10; **c**: $p < 0.05$ vs. Celecoxib; **Control:** 0.3% w/v sodium CMC in distilled water (10 ml/kg, *p.o.*); **Indo 10:** Indomethacin (10 mg/kg, *p.o*) in 0.3% w/v sodium CMC; **Celecoxib** and other test compounds were administered in 0.3% w/v sodium CMC at an equimolar oral dose relative to 10 mg/kg indomethacin.

5.B.2.2. Evaluation of Analgesic Activity

5.B.2.2.1. Acetic Acid-Induced Writhing in Mice

The outcome of the acetic acid induced writhing in mice is summarised in **Table 5.20**. In mice, oral administration of compounds **$S_2$2c-$S_2$2e** and **$S_2$3c-$S_2$3e** thirty minutes before acetic acid injection produced a significant ($p < 0.05$) inhibition of the abdominal constrictions induced by the acetic acid. Indomethacin and celecoxib which are non-selective and selective COX-2 inhibitors respectively also reduced significant inhibition of the response to acetic acid writhing.

TABLE 5.20. Acetic Acid Induced Writhing

Compound	Total no. of writhings	% Inhibition
Control	62.28 ± 4.48	--
Indo 10	15.15 ± 1.17^{a}	75.67
Celecoxib	16.67 ± 1.22^{a}	73.23
$S_2$2c	18.87 ± 1.33^{ac}	69.70
$S_2$2d	18.17 ± 1.25^{a}	70.82
$S_2$2e	18.56 ± 1.28^{a}	70.20
$S_2$3c	19.72 ± 1.35^{ac}	68.34
$S_2$3d	20.28 ± 1.29^{ac}	67.44
$S_2$3e	19.42 ± 1.37^{ac}	68.82

Values are expressed as the Mean ± S.D (n = 6); **a**: $p < 0.05$ vs. Control; **c**: $p < 0.05$ vs. Celecoxib; **Control:** 0.3% w/v sodium CMC in distilled water (10 ml/kg, *p.o.*); **Indo 10:** Indomethacin (10 mg/kg, *p.o*) in 0.3% w/v sodium CMC; **Celecoxib** and other test compounds were administered in 0.3% w/v sodium CMC at an equimolar oral dose relative to 10 mg/kg indomethacin.

antihistaminic (Yeh, 1985) can also inhibit the writhes induced by acetic acid. To avoid misinterpretation of the results, the anti-nociceptive effects of the compounds were further confirmed using the formalin bioassay model.

5.B.2.2.2. Formalin-Induced Paw Licking in Mice

This model consists of two distinct phases. The first phase represents the irritating effects of formalin at the sensorial fibres-C. The second is an inflammatory pain response. Centrally acting analgesics such as pentazocine inhibit both phases. Peripheral acting drugs such as NSAID's inhibit only the second phase. The compounds **(S_22c-S_22e** and **S_23c-S_23e)** were subjected to formalin-induced paw licking in mice for estimation of analgesic activity, and the result is summarised in **Table 5.21**.

TABLE 5.21. Formalin-Induced Paw Licking

Compound	**Time spent in licking (sec)**		**% Inhibition**	
	Phase I (0–10 min)	**Phase II (15–30 min)**	**Phase I (0–10 min)**	**Phase II (15–30 min)**
Control	102.33 ± 7.68	115.70 ± 8.77	–	–
PTZ 10	14.73 ± 1.09^{a}	13.14 ± 0.82^{a}	85.60	88.64
Indo 10	83.66 ± 5.42^{ab}	18.85 ± 0.91^{a}	18.24	83.71
Celecoxib	86.49 ± 6.30^{ab}	22.95 ± 1.53^{ab}	15.48	80.16
S_22c	88.04 ± 7.10^{ab}	24.34 ± 1.69^{ab}	13.96	78.96
S_22d	87.57 ± 6.22^{ab}	23.12 ± 1.57^{ab}	14.42	80.02
S_22e	89.25 ± 7.05^{ab}	23.32 ± 1.64^{ab}	12.78	79.84
S_23c	90.18 ± 7.18^{ab}	25.73 ± 1.73^{abc}	11.87	77.76

The inhibitory effect of hybrids **S$_2$2c-S$_2$2e** and **S$_2$3c-S$_2$3e** in the late phase of the formalin test suggests that its anti-nociceptive activity is due, at least in part, to an anti-inflammatory action. Their anti-nociceptive effect is attributed to the inhibition of COX-2 thereby halting the release of prostanoids, which contributes to the development of peripheral sensitisation through phosphorylation of ion channels in the nociceptor terminals, increasing excitability and reducing the pain threshold (McCleskey and Gold, 1999). The fact that the compounds elicited an anti-nociceptive effect on the late phase suggests that they do not block the neural transmission of pain in a way that pentazocine does.

5.B.2.3. *In Vitro* COX Inhibition Assay

Compounds **S$_2$2c-S$_2$2e** and **S$_2$3c-S$_2$3e** were evaluated *in vitro* against COX-1 and COX-2 to determine the IC$_{50}$ values and ascertain their specificity. The result of the *in vitro* COX inhibition assay is presented in **Table 5.22**.

TABLE 5.22. COX Inhibitory Activity and Selectivity Index (COX–1/COX–2) of Selected Compounds

Compound	**IC$_{50}$ (µM)^a**		**COX-2 Selectivity index^b**	**Type of Inhibition for COX-2**	**COX-2 K_i (µM)**
	COX-1	**COX-2**			
S$_2$2c	60.54 ± 4.38^g	0.77 ± 0.023^g	78.62	competitive	0.65
S$_2$2d	64.53 ± 4.12^g	0.65 ± 0.028^g	99.28	competitive	0.63
S$_2$2e	62.44 ± 3.77^g	0.60 ± 0.025^g	104.07	competitive	0.50
S$_2$3c	60.06 ± 3.89^g	0.90 ± 0.037^g	66.73	competitive	0.77
S$_2$3d	62.19 ± 4.42^g	1.11 ± 0.075^g	56.03	competitive	0.96
S$_2$3e	63.17 ± 3.82^g	1.01 ± 0.068^g	63.54	competitive	0.88

Amongst the estimated compounds, the 1,2,4-oxadiazole derivative bearing a 4-nitrophenyl substitution **(S$_2$2e)** and its 4-chlorophenyl counterpart **(S$_2$2d)** were the most potent COX-2 inhibitors with IC$_{50}$ values of 0.60 μM and 0.65 μM**,** respectively. As evidenced by the IC$_{50}$ and selectivity index data, unlike indomethacin, a non-selective COX inhibitor (SI = 1.03), these compounds displayed higher selectivity towards the inhibition of COX-2 over COX-1 which confirmed their selective COX-2 inhibitory potential. It also explains their improved gastric tolerability on prolonged use. However, selective COX-2 selective inhibitors are associated with cardiovascular side effects, which have led to the voluntary withdrawal of drugs such as rofecoxib (Vioxx®) from the market. This augurs for the evaluation of cardiotoxic liability of the synthesised potent selective COX-2 inhibitor to establish its cardiac safety.

5.B.2.3.1. Enzyme Kinetics Study

Furthermore, substrate dependent kinetic parameters were determined to characterise the mechanism of inhibition of COX-2 isoform by compounds **S$_2$2c-S$_2$2e** and **S$_2$3c-S$_2$3e**. The kinetic parameters of the present study were determined based on Michaelis-Menten equation followed by a Lineweaver-Burk double reciprocal analysis of dataset regarding 1/V$_{max}$ Vs 1/[S] plot.

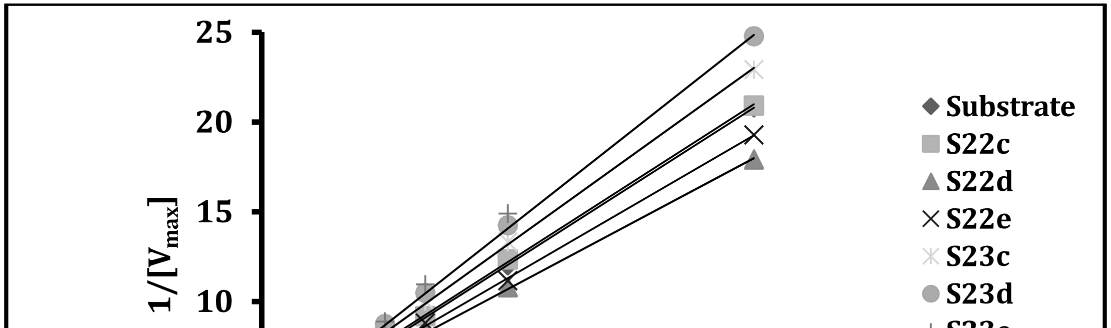

As shown in **Fig. 5.13**, the slopes of the Lineweaver-Burk plots of each of the promising compounds are different. Yet, the $1/V_{max}$ (*y-intercept*) values for compounds **$S_2$2c-$S_2$2e** and **$S_2$3c-$S_2$3e** the same confirming their competitive inhibitory nature for COX-2 on its substrate arachidonic acid.

5.B.2.4. Evaluation of Cardiotoxic Liability

Based on the outcome of the *in vitro* COX inhibition assay study, the most potent compound from the 1,3,4-oxadiazole series **($S_2$2e)** and 1,3,4-thiadiazole series **($S_2$3c)** was selected and evaluated for their cardiotoxic liability in myocardial infarcted rats. Serum levels of biomarkers such as Cardiac troponin I (cTnI) and Creatine kinase-MB (CK-MB) are useful in establishing the diagnosis of myocardial infarction (Nigam, 2007).

It has been reported that ISO causes myocardial infarction (MI) by increasing the levels of cTnI and CK-MB in the serum of the animals (Stanley and Roy, 2013; Kumar *et al.*, 2016a) and is a well-developed non-invasive animal model of MI (Kannan and Quine, 2013). The advantage of this model over surgical method lies in its simplicity, non-invasive technique thus no chance of contracting post- surgical infections and a low mortality rate.

The pattern of ischemic necrosis ISO-induced MI is analogous to humans because it produces maximum necrosis in the ventricular subendocardial region and inter-ventricular septum (Kumar *et al.*, 2016b). Alteration in serum levels of cardiac injury biomarkers (cTnI and CK-MB) in both normal and ISO-induced MI in rats are summarised in **Tables 5.23** & **5.24**.

Administration of ISO resulted in a significant increase ($p < 0.05$) in serum

TABLE 5.23. Effects of Celecoxib, **$S_2$2e** and **$S_2$3c** on the Levels of cTnI on ISO Induced Myocardial Infarcted Rats

Treatment	**cTnI levels (ng/ml)**					
	Day 0	**Day 3**	**Day 4**	**Day 7**	**Day 11**	**Day 19**
Normal Control	0.58± 0.044	0.55± 0.040	0.57± 0.041	0.57± 0.045	0.58± 0.045	0.57± 0.043
ISO Control	0.67± 0.050	2.82± 0.198^a	1.90± 0.138^a	0.92± 0.037^a	0.70± 0.029	0.69± 0.032
ISO+ Celecoxib	0.58± 0.030	2.88± 0.192^a	1.78± 0.122^a	0.84± 0.030^a	0.69± 0.033	0.68± 0.028
ISO+ $S_2$2e	0.56± 0.022	2.90± 0.195^a	1.82± 0.127^a	0.80± 0.028^a	0.68± 0.030	0.58± 0.028
ISO+ $S_2$3c	0.54± 0.038	2.92± 0.191^a	1.77± 0.134^a	0.85± 0.033^a	0.62± 0.027	0.60± 0.022

Values are expressed as the Mean ± S.D (n = 6); **a**: $p < 0.05$ vs. Control; **Normal Control:** 0.3% w/v sodium CMC solution in distilled water (10 ml/kg, *p.o.*); **ISO Control:** Isoproterenol (100 mg/kg, *s.c.*); Compounds (Celecoxib, **$S_2$2e** and **$S_2$3c**) were administered in 0.3% w/v sodium CMC at an equimolar oral dose relative to 10 mg/kg indomethacin.

TABLE 5.24. Effects of Celecoxib, **$S_2$2e** and **$S_2$3c** on the Levels of CK-MB on ISO Induced Myocardial Infarcted Rats

Treatment	**CK-MB levels (ng/ml)**					
	Day 0	**Day 3**	**Day 4**	**Day 7**	**Day 11**	**Day 19**
Normal Control	14.24± 0.92	14.29± 0.99	14.27± 0.98	14.25± 0.95	14.25± 0.97	14.26± 0.93
ISO Control	15.57± 1.12	102.30± 7.34^a	70.26± 4.42^a	32.68± 1.98^a	17.86± 1.26	17.22± 1.21
ISO+ Celecoxib	15.42± 1.17	100.78± 7.88^a	72.32± 5.04^a	35.15± 2.04^a	17.63± 1.11	17.17± 1.19
ISO+ $S_2$2e	14.84± 1.12	98.69± 6.79^a	69.28± 4.42^a	31.33± 2.16^a	15.29± 1.23	15.02± 1.30
ISO+ $S_2$3c	14.68± 1.20	100.72± 7.42^a	69.43± 4.88^a	33.57± 2.08^a	16.75± 1.33	16.13± 1.37

Values are expressed as the mean ± S.D (n = 6); **a**: $p < 0.05$ vs. Control; **Normal Control:**

5.B.3. COMPUTATIONAL STUDIES

5.B.3.1. *In Silico* Docking

Molecular docking studies were performed using the GLIDE (Grid-Based Ligand Docking with Energetics) extra precision (XP) programme to gain insight into the possible mode of protein-ligand interaction at the COX-2 active site. Validation of docking experiment was performed by using the superposition tool in Schrödinger Maestro 10.5.014 on the mouse COX-2 enzyme (PDB ID: 3LN1) with celecoxib as the co-crystallised ligand. Since the data on murine COX-2 have been reported in the study involving selected potential compounds from Series 1, the numbers of amino acid residues in murine COX-2 analogue are written in parenthesis for easy comparison with crystallographic data and docking results presented in the Series 1 and elsewhere in reported literatures. The affinity of selective inhibitors is mainly governed by the hydrophobic interactions within the confined COX-2 binding pocket (Kurumbail *et al.*, 1996; Wang *et al.,* 2010).

The RMSD (root mean square deviation) value equal to 0.318 Å (**Fig. 5.14**) suggested that predicted and actual crystallographic conformation of celecoxib were within the acceptable limit of 2 Å (Kontoyianni *et al.*, 2004). It confirmed that the parameters set for Glide-XP docking mode were reliable in generating reproducible *in silico* binding mode for COX-2 inhibitors. The result of the docking study is depicted in **Table 5.25**.

The potent compounds **$S_2$2e** (IC$_{50}$: 0.60 μM) (GLIDE Score: -11.95); **$S_2$2d** (IC$_{50}$: 0.65 μM) (GLIDE Score: -11.72) and **$S_2$2c** (IC$_{50}$: 0.77 μM) (GLIDE Score: -10.82) exhibited a Y-shaped structure wherein the biphenyl rings stretched effectively to interact with the hydrophobic amino acid residues Ile 503 (517), Arg 499 (513), Ala 502 (516), Val 509 (523), Leu 338 (352), Met 508 (522), and

Table 5.25. Glide Score and Docking Interactions of Selected Potential Compounds.

Sr. No.	Ligand	Glide Score	Amino acid interactions at the COX-2 active site
01	**$S_2$2c**	-10.82	His 75 (90), Gln 178 (192), Ser 339 (353), Tyr 341 (355), Leu 345 (359), Arg 499 (513), Ala 502 (516), Phe 504 (518), Val 509 (523)
02	**$S_2$2d**	-11.72	His 75 (90), Gln 178 (192), Ser 339 (353), Tyr 341 (355), Arg 499 (513), Asp 501 (515), Ile 503 (517), Phe 504 (518), Val 509 (523)
03	**$S_2$2e**	-11.95	His 75 (90), Gln 178 (192), Leu 338 (352), Ser 339 (353), Arg 499 (513), Asp 501 (515), Ala 502 (516), Ile 503 (517), Phe 504 (518), Val 509 (523)
04	**$S_2$3c**	-8.00	His 75 (90), Gln 178 (192), Val 335 (349), Ser 339 (353), Tyr 341 (355), Arg 499 (513), Ala 502 (516Val 509 (523), Ala 513 (527), Leu 517 (531)
05	**$S_2$3d**	-8.00	His 75 (90), Gln 178 (192), Val 335 (349), Ser 339 (353), Tyr 341 (355), Arg 499 (513), Ala 502 (516), Phe 504 (518), Val 509 (523), Ala 513 (527), Leu 517 (531)
06	**$S_2$3e**	-7.10	His 75 (90), Gln 178 (192), Val 335 (349), Ser 339 (353), Tyr 341 (355), Arg 499 (513), Ala 502 (516), Phe 504 (518), Val 509 (523), Ala 513 (527), Leu 517 (531)

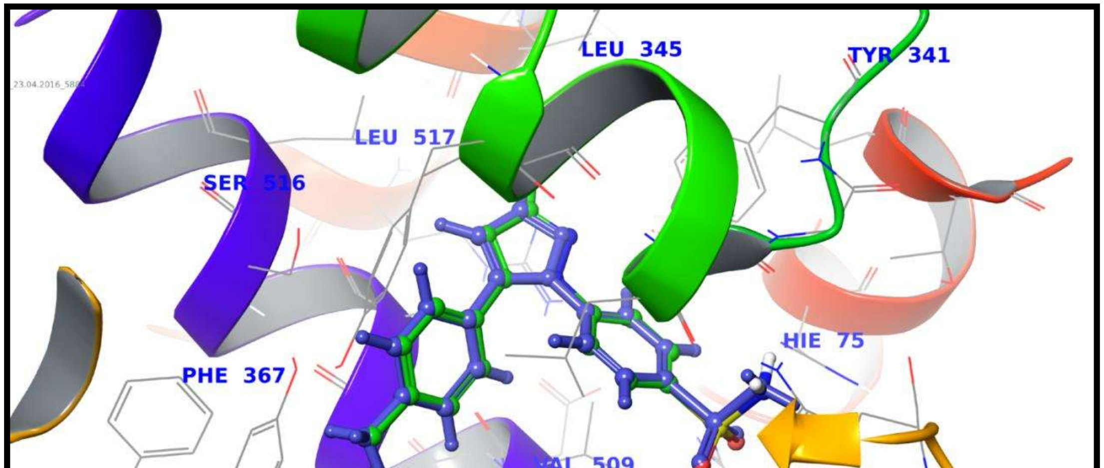

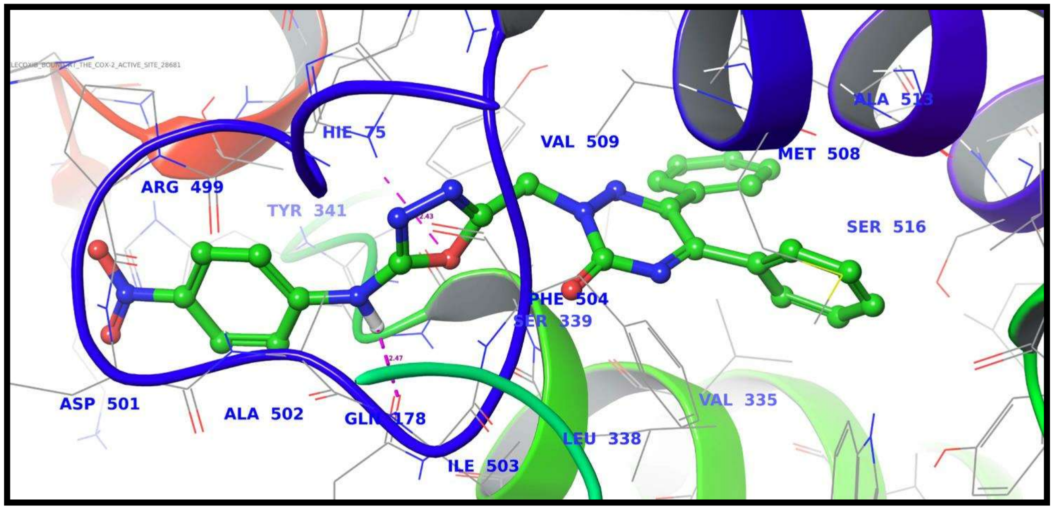

Figure 5.15. 3D view of the docking study of the minimum energy structure of the complex of **$S_2$2e** docked in COX-2 (PDB: 3LN1).

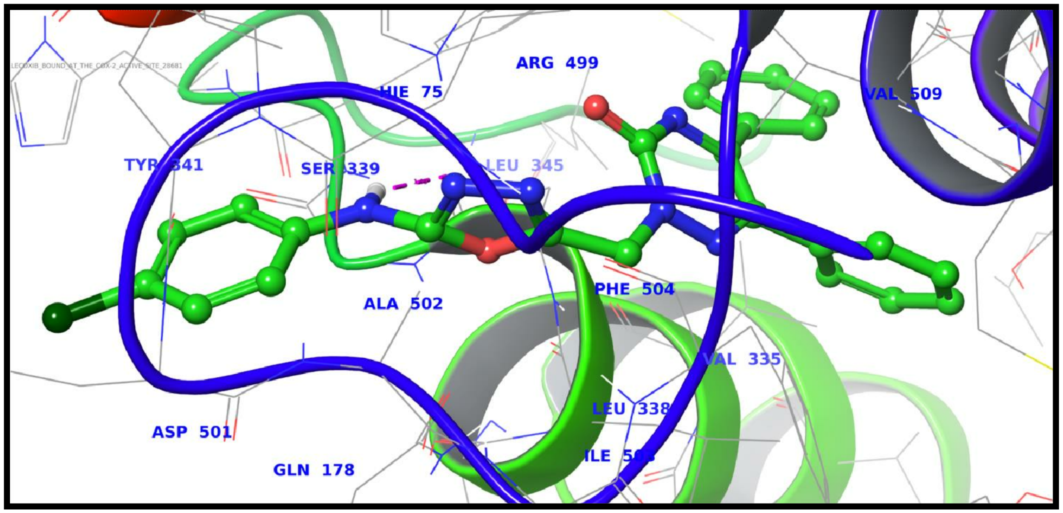

Figure 5.16. 3D view of the docking study of the minimum energy structure of the complex of **$S_2$2d** docked in COX-2 (PDB: 3LN1).

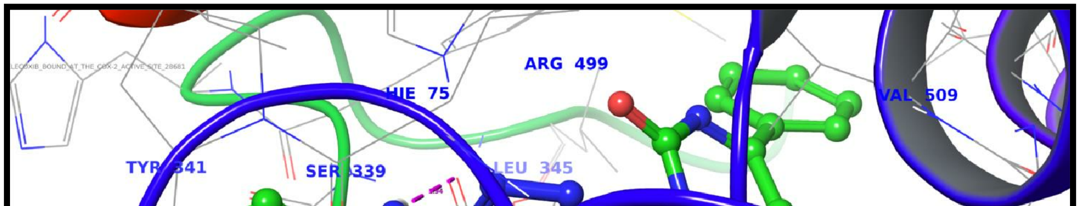

The compound **S$_2$2e** revealed that hydrogen bond interaction between the oxygen atom of the 1,3,4-oxadiazole ring and His 75 (90) was (2.43 Å). Another hydrogen bond was observed between the -NH linker of **S$_2$2e** and Gln 178 (192) (2.47 Å). For compound **S$_2$2d**, hydrogen bonding (1.94 Å) was found between Ser 339 (353) and the -NH linker group. Similarly, for compound **S$_2$2e**, hydrogen bonding interaction (1.94 Å) was observed between Ser 339 (353) and the -NH linker group.

The outcome of the docking exercise thus exemplified the consensual interaction of the docked ligand within the COX-2 active site. It was notable that the compounds (**S$_2$4a-S$_2$4e**) failed to dock into the COX-2 active site even after the docking parameters were relaxed to an extent. Further investigation into this phenomenon revealed that the peculiar L-shaped spatial arrangement of their minimum energy conformer (**Fig. 5.18**) compounded with the absence of -NH linker increased their overall rigidity. It also restricted their entry into the COX-2 active site and subsequent interaction with the active amino acids.

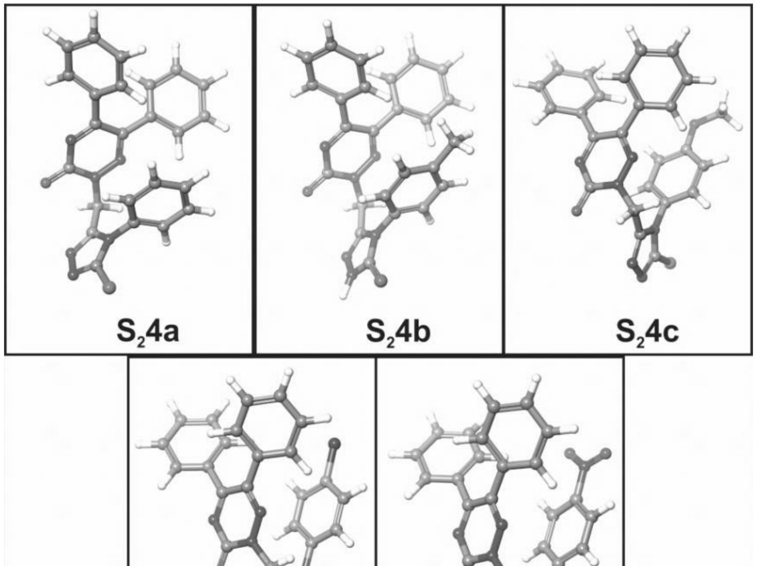

oedema model. From this, one infer that not merely the presence of a particular pharmacophoric group but the rigid three-dimensional arrangement of its minimum energy conformer seem to get further aggravated by the absence of the –NH linker coupled with the aromatic planar moiety as observed in the case of compounds **$S_2$4a-$S_2$4e** was responsible for their diminished anti-inflammatory effect.

5.B.3.2. *In silico* molecular dynamics (MD)

A 20 ns MD simulation of the solvated energy minimised docked complex of compound **$S_2$2e** (also referred as 'ligand'), and COX-2 (PDB ID: 3LN1) was performed post-docking studies for the assessment of predicted binding mode. The overall stability of the system was evaluated by RMSD (Root mean square deviation) calculations. RMSD values confirmed that all frames of the complex were in trajectory throughout the experiment when the atom of a particular frame was compared with the reference frame. The RMSD plot indicated that the protein backbone was stable through the phase of MD simulation and attained the equilibrium within 1.2 ns with an average fluctuation of 1 Å (**Fig. 5.19**).

A graphical examination of **Fig. 5.20** confirmed the binding of compound **$S_2$2e** with the active amino acid residues in the COX-2 site. The snapshot revealed that the compound **$S_2$2e** efficiently interacted through water bridges to form H-bond with critical polar amino acid residues His 75 (90) and Tyr 341 (355). Besides, it also interacted with other essential amino acids such as Arg 106 (120), Leu 338 (352), Val 335 (349) and Ala 513 (527) surrounding the COX-2 pocket through hydrophobic interactions.

Protein interactions with compound **$S_2$2e** were analysed and calculated as

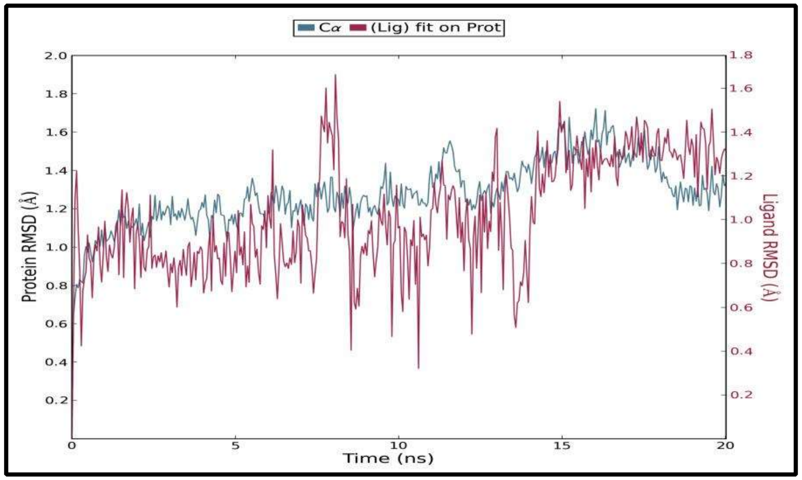

Figure 5.19. Protein–ligand RMSD. RMSD evaluation of a protein (left *Y*–axis); the ligand RMSD (right *Y*–axis) indicating the stability of ligand **$S_2$2e** with respect to the protein and its binding pocket

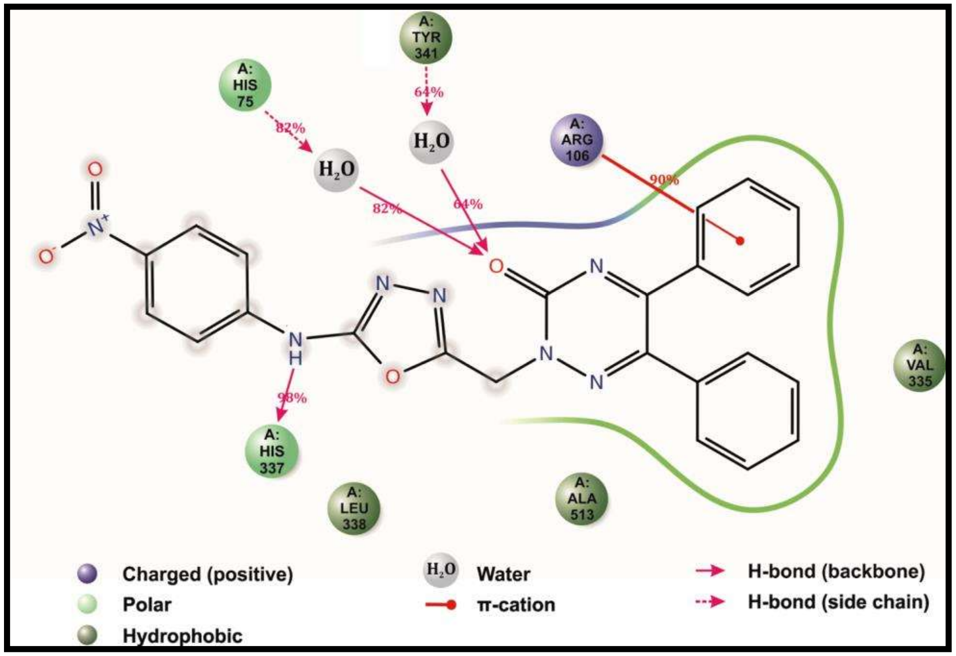

Figure 5.20. The detailed atomic interactions of ligand **$S_2$2e** with the key amino acid residues at the COX-2 active site.

The MD simulations of COX-2 with a low micromolar inhibitor (compound **$S_2$2e**) reasserted its dynamic stability throughout the simulation run. It also substantiated that the binding interactions predicted by docking studies were stable. This exercise reaffirmed the selective COX-2 inhibition of the compound **$S_2$2e** and its anti-inflammatory activity.

5.B.3.3. Estimation of "Drug-Like" Properties

Prediction of "drug-likeliness" for the most active compounds was carried out using QikProp module of Schrödinger Maestro 10.5.014. The predicted outcome of some important parameters including Log P is reported in **Table 5.26**. The experimental Log P values (**Table 5.13**) were found in the range of 3.44-4.58 with the mean Log P value of 4.10 and vary with those predicted *in silico*. The experimental Log P values conform to ≤ 5 which is in compliance with Lipinski's rule of five (Lipinski *et al.*, 2001) to ascertain whether a chemical compound with certain pharmacological activity is endowed with properties that would make it a likely orally active drug in humans.

Amongst the calculated parameters, the number of rotatable bonds (#rotor) provides a prediction for the conformational flexibility of the molecule, which in turn, decides the binding to its target protein. Polar surface area (PSA) is another important parameter used in estimating the drug transporter properties. PSA is the sum of surfaces of polar atoms such as oxygen, nitrogen, and attached hydrogen. Along with Lipinski's rule of five, these two parameters are vital in achieving a good oral bioavailability (Veber *et al.*, 2002).

Of the other predicted parameter, QPPCaco predicts for the non-active transport for the gut-blood barrier using Caco-2 cells as a model. It reflects the

TABLE 5.26. Predicted Drug Likeliness Properties for the Most Active Compounds

Compound	Mol_MW (130-725)	#rotor (0-15)	PSA (7-200)	donorHB (0-6)	accptHB (2-20)	QPlogPo/w (-2-6.5)	QPP Caco (<25 poor, >500 great)	QPlogKhsa (-1.5-1.5)	% Human oral absorption >80% high, <25% poor)	Rule of five (Max 4)
S$_2$2c	452.47	8	19.37	1	6.75	4.84	696.47	0.669	100.00	0
S$_2$2d	456.89	7	101.11	1	6.00	5.28	725.87	0.789	96.10	1
S$_2$2e	467.44	8	146.00	1	7.00	4.05	83.31	0.611	72.08	1
S$_2$3c	468.53	8	97.61	1	6.25	5.54	953.73	0.875	100.00	1
S$_2$3d	472.95	7	89.28	1	5.50	5.94	914.51	0.994	100.00	1
S$_2$3e	483.50	8	134.22	1	6.50	4.73	109.31	0.816	91.13	0

Mol_MW: molecular weight; **#rotor:** No. of rotatable bonds; **donorHB:** No. of hydrogen bonds that would be donated by the solute to water molecules in an aqueous solution; **accptHB:** No. of hydrogen bonds that would be accepted by the solute from water molecules in an aqueous solution; **QPlogPo/w:** Predicted octanol/water partition coefficient; **QPPCaco:** Caco-2 cell permeability in nm/sec; **QPlogKhsa:** binding to human serum albumin; **Percentage Human-Oral Absorption:** human oral absorption on 0 to 100% scale; **PSA:** polar surface area; **Rule of Five:** No. of violations of Lipinski's rule of five.

All the compounds under study displayed a good human (72-100%) oral absorption. The outcome of Lipinski's rule of five (mol_MW < 500, QPlog Po/w < 5, donorHB 0-6.0, accptHB 2.0-20), along with the other predicted parameters indicated that the compounds under consideration (**$S_2$2c-$S_2$2e** and **$S_2$3c-$S_2$3e**) did elicit "drug-like" characteristics.

TABLE 5.15. Carrageenan-Induced Paw Oedema

Compound	**Swelling thickness in mm (% Inhibition)**						
	0 h	**1 h**	**2 h**	**3 h**	**4 h**	**5 h**	**6 h**
Control	3.23 ± 0.26	8.02 ± 0.63	8.68 ± 0.67	8.80 ± 0.64	8.72 ± 0.68	8.48 ± 0.63	8.23 ± 0.68
Indo 10	3.02 ± 0.21	3.59 ± 0.23^{a} (55.24)	3.60 ± 0.27^{a} (58.52)	3.30 ± 0.22^{a} (62.50)	3.21 ± 0.25^{a} (63.19)	3.09 ± 0.28^{a} (63.56)	3.26 ± 0.19^{a} (60.39)
Celecoxib	3.12 ± 0.20	3.75 ± 0.30^{a} (53.24)	3.81 ± 0.35^{a} (56.11)	3.35 ± 0.31^{a} (61.93)	3.23 ± 0.29^{a} (62.96)	3.20 ± 0.22^{a} (62.26)	3.19 ± 0.30^{a} (61.24)
$S_2$2c	3.19 ± 0.29	5.04 ± 0.45^{abc} (37.16)	4.84 ± 0.44^{abc} (44.24)	3.93 ± 0.36^{ab} (55.34)	3.51 ± 0.32^{a} (59.75)	3.32 ± 0.25^{a} (60.85)	3.29 ± 0.29^{a} (60.02)
$S_2$2d	3.07 ± 0.23	4.91 ± 0.45^{abc} (38.78)	4.68 ± 0.41^{abc} (46.08)	3.74 ± 0.32^{a} (57.50)	3.53 ± 0.29^{a} (59.52)	3.31 ± 0.23^{a} (60.97)	3.28 ± 0.31^{a} (60.14)
$S_2$2e	3.19 ± 0.27	4.95 ± 0.42^{abc} (38.28)	4.76 ± 0.44^{abc} (45.16)	3.58 ± 0.31^{a} (59.32)	3.45 ± 0.29^{a} (60.43)	3.26 ± 0.28^{a} (61.56)	3.26 ± 0.24^{a} (60.39)
$S_2$3c	3.24 ± 0.20	5.20 ± 0.50^{abc} (35.16)	4.97 ± 0.47^{abc} (42.74)	3.94 ± 0.35^{ab} (55.23)	3.56 ± 0.31^{a} (59.17)	3.46 ± 0.20^{a} (59.20)	3.43 ± 0.33^{a} (58.32)
$S_2$3d	3.31 ± 0.28	5.31 ± 0.46^{abc} (33.79)	5.20 ± 0.48^{abc} (40.10)	4.07 ± 0.36^{abc} (53.75)	3.75 ± 0.34^{a} (56.99)	3.57 ± 0.31^{a} (57.90)	3.59 ± 0.33^{a} (56.38)
$S_2$3e	3.15 ± 0.22	5.07 ± 0.43^{abc} (36.78)	4.79 ± 0.37^{abc} (44.81)	3.92 ± 0.33^{ab} (55.45)	3.63 ± 0.31^{a} (58.37)	3.52 ± 0.30^{a} (58.49)	3.36 ± 0.32^{a} (59.17)
$S_2$4d	3.28 ± 0.22	5.74 ± 0.52^{abc} (28.43)	6.05 ± 0.58^{abc} (30.30)	5.38 ± 0.44^{abc} (38.86)	4.98 ± 0.36^{abc} (42.89)	4.80 ± 0.39^{abc} (43.40)	4.71 ± 0.45^{abc} (42.77)
$S_2$4e	3.45 ± 0.28	6.01 ± 0.41^{abc} (25.06)	6.18 ± 0.40^{abc} (28.80)	6.18 ± 0.55^{abc} (29.77)	5.82 ± 0.52^{abc} (33.26)	5.25 ± 0.49^{abc} (38.09)	5.29 ± 0.43^{abc} (35.72)

Values are expressed as the Mean ± S.D (n = 6).; **a**: $p < 0.05$ vs. Control; **b**: $p < 0.05$ vs. Indo; **c**: $p < 0.05$ vs. Celecoxib; **Control:** 0.3% w/v sodium in distilled water (10 ml/kg, *p.o.*); **Indo 10:** Indomethacin (10 mg/kg, *p.o*) in 0.3% w/v sodium CMC; **Celecoxib** and other test compounds were administered in 0.3% w/v sodium CMC at an equimolar oral dose relative to 10 mg/kg indomethacin.

TABLE 5.18. Adjuvant-Induced Arthritis, Ulcer Index and Lipid Peroxidation

Comp.	Paw thickness (mm)							Ulcer Index ± S.D	nmol for MDA content ± S.D 100 mg^{-1} tissue
	Day 03	Day 06	Day 09	Day 12	Day 15	Day 18	Day 21		
Control	7.92 ± 0.58	8.10 ± 0.62	8.32 ± 0.60	8.38 ± 0.64	8.44 ± 0.60	8.51 ± 0.63	8.56 ± 0.61	0	4.24 ± 0.34
Indo 10	5.53 ± 0.40^{a} (30.18)	4.96 ± 0.42^{a} (38.77)	4.62 ± 0.42^{a} (44.47)	4.47 ± 0.41^{a} (46.66)	3.96 ± 0.35^{a} (53.08)	3.54 ± 0.33^{a} (58.40)	3.45 ± 0.31^{a} (59.70)	55 ± 3.8	8.38 ± 0.57^{a}
Celecoxib	5.44 ± 0.46^{a} (31.31)	5.11 ± 0.43^{a} (36.91)	4.96 ± 0.34^{a} (40.38)	4.76 ± 0.41^{a} (43.20)	4.25 ± 0.40^{a} (49.64)	3.99 ± 0.35^{a} (53.11)	3.77 ± 0.32^{a} (55.96)	26 ± 1.9	6.82 ± 0.54^{ab}
$S_2$2c	5.67 ± 0.47^{a} (28.41)	5.53 ± 0.52^{ab} (31.73)	5.09 ± 0.44^{a} (38.82)	4.90 ± 0.42^{a} (41.53)	4.57 ± 0.43^{a} (45.85)	4.41 ± 0.40^{ab} (48.18)	4.14 ± 0.38^{a} (51.64)	22 ± 1.8	4.67 ± 0.35^{abc}
$S_2$2d	5.77 ± 0.55^{a} (27.15)	5.64 ± 0.43^{a} (30.37)	5.23 ± 0.46^{a} (37.14)	4.94 ± 0.41^{a} (41.05)	4.48 ± 0.37^{a} (46.92)	4.33 ± 0.41^{ab} (49.12)	4.09 ± 0.36^{a} (52.22)	20 ± 1.1	4.18 ± 0.37^{abc}
$S_2$2e	5.52 ± 0.42^{a} (30.30)	5.35 ± 0.47^{a} (33.95)	5.05 ± 0.45^{a} (39.30)	4.68 ± 0.41^{a} (44.15)	4.28 ± 0.39^{a} (49.29)	3.96 ± 0.36^{a} (53.47)	3.83 ± 0.35^{a} (55.26)	24 ± 2.0	4.31 ± 0.39^{abc}
$S_2$3c	5.74 ± 0.48^{a} (27.53)	5.66 ± 0.43^{ab} (30.12)	5.40 ± 0.31^{ab} (35.10)	4.85 ± 0.43^{a} (42.12)	4.70 ± 0.40^{ab} (44.31)	4.39 ± 0.38^{ab} (48.41)	4.12 ± 0.28^{a} (51.87)	23 ± 1.5	4.54 ± 0.38^{abc}
$S_2$3d	5.57 ± 0.51^{a} (29.67)	5.44 ± 0.41^{a} (32.84)	5.35 ± 0.43^{ab} (35.70)	5.11 ± 0.45^{a} (39.02)	4.83 ± 0.47^{ab} (42.77)	4.45 ± 0.42^{ab} (47.71)	4.20 ± 0.37^{ab} (50.93)	24 ± 2.2	4.83 ± 0.33^{abc}
$S_2$3e	5.68 ± 0.54^{a} (28.28)	5.62 ± 0.48^{a} (30.62)	5.30 ± 0.50^{a} (36.30)	4.90 ± 0.30^{a} (41.53)	4.72 ± 0.42^{ab} (44.08)	4.47 ± 0.41^{ab} (47.47)	4.18 ± 0.28^{ab} (51.17)	22 ± 1.3	5.02 ± 0.41^{abc}

Values are expressed as the Mean ± S.D (n = 6); **a**: $p < 0.05$ vs. Control; **b**: $p < 0.05$ vs. Indo 10; **c**: $p < 0.05$ vs. Celecoxib; **Control:** 0.3% w/v sodium CMC in distilled water (10 ml/kg, *p.o.*); **Indo 10:** Indomethacin (10 mg/kg, *p.o*) in 0.3% w/v sodium CMC; **Celecoxib** and other test compounds were administered in 0.3% w/v sodium CMC at an equimolar oral dose relative to 10 mg/kg indomethacin.

TABLE 5.19. Effect of Selected Potential Compounds on Hepatic and Renal Toxicity Parameters as Evaluated on 21st Day after Treatment

Compound	SGOT (U/mL)	SGPT (U/mL)	ALP (U/mL)	Total protein (g/dL)	Total albumin (g/dL)	CR (mg/dL)	BUN (mg/dL)
Control	90.87 ± 6.38	31.36 ± 2.20	18.12 ± 0.96	1.91 ± 0.13	1.62 ± 0.09	0.58 ± 0.039	21.88 ± 1.42
Indo 10	118.68 ± 8.23^{a}	51.34 ± 3.91^{a}	27.18 ± 1.53^{a}	2.32 ± 0.15^{a}	2.48 ± 0.17^{a}	1.91 ± 0.12^{a}	63.17 ± 1.54^{a}
Celecoxib	113.56 ± 8.38^{a}	48.33 ± 3.65^{a}	25.83 ± 1.68^{a}	2.21 ± 0.15^{a}	2.30 ± 0.14^{a}	1.32 ± 0.07^{ab}	61.38 ± 1.49^{a}
$S_2$2c	97.89 ± 7.68^{bc}	38.11 ± 3.09^{abc}	20.67 ± 1.23^{bc}	2.02 ± 0.14^{b}	1.82 ± 0.14^{bc}	0.91 ± 0.05^{abc}	42.78 ± 1.32^{abc}
$S_2$2d	98.77 ± 7.42^{bc}	41.34 ± 3.15^{abc}	21.34 ± 1.55^{abc}	2.03 ± 0.17^{b}	1.92 ± 0.15^{abc}	1.17 ± 0.07^{abc}	45.78 ± 1.36^{abc}
$S_2$2e	98.12 ± 7.18^{bc}	38.88 ± 2.94^{abc}	20.97 ± 1.56^{abc}	1.98 ± 0.13^{b}	1.88 ± 0.16^{bc}	1.04 ± 0.07^{abc}	45.17 ± 1.36^{abc}
$S_2$3c	96.91 ± 6.98^{bc}	40.20 ± 3.34^{abc}	21.09 ± 1.62^{abc}	2.00 ± 0.12^{b}	1.96 ± 0.17^{abc}	0.95 ± 0.06^{abc}	47.24 ± 1.34^{abc}
$S_2$3d	97.23 ± 7.07^{bc}	39.78 ± 3.11^{abc}	22.11 ± 1.66^{abc}	1.97 ± 0.16^{b}	1.87 ± 0.18^{bc}	1.08 ± 0.05^{abc}	48.71 ± 1.41^{abc}
$S_2$3e	97.88 ± 7.41^{bc}	41.97 ± 3.57^{abc}	22.54 ± 1.60^{abc}	2.00 ± 0.18^{b}	1.95 ± 0.17^{abc}	1.20 ± 0.08^{abc}	49.83 ± 1.40^{abc}

SGOT: Serum Glutamic Oxaloacetic Transaminase; **SGPT:** Serum Glutamic Pyruvic Transaminase; **ALP:** Alkaline Phosphatase; **CR:** Creatinine; **BUN:** Blood Urea Nitrogen; Values are expressed as the Mean ± S.D (n = 6); **a**: $p < 0.05$ vs. Control; **b**: $p < 0.05$ vs. Indo 10; **c**: $p < 0.05$ vs. Celecoxib; **Control:** 0.3% w/v sodium CMC in distilled water (10 ml/kg, *p.o.*); **Indo 10:** Indomethacin (10 mg/kg, *p.o*) in 0.3% w/v sodium CMC; **Celecoxib** and other test compounds were administered in 0.3% w/v sodium CMC at an equimolar oral dose relative to 10 mg/kg indomethacin.

TABLE 5.26. Predicted Drug Likeliness Properties for the Most Active Compounds

Compound	Mol_MW (130-725)	#rotor (0-15)	PSA (7-200)	donorHB (0-6)	accptHB (2-20)	QPlogPo/w (-2-6.5)	QPP Caco (<25 poor, >500 great)	QPlogKhsa (-1.5-1.5)	% Human oral absorption >80% high, <25% poor)	Rule of five (Max 4)
$S_2$2c	452.47	8	19.37	1	6.75	4.84	696.47	0.669	100.00	0
$S_2$2d	456.89	7	101.11	1	6.00	5.28	725.87	0.789	96.10	1
$S_2$2e	467.44	8	146.00	1	7.00	4.05	83.31	0.611	72.08	1
$S_2$3c	468.53	8	97.61	1	6.25	5.54	953.73	0.875	100.00	1
$S_2$3d	472.95	7	89.28	1	5.50	5.94	914.51	0.994	100.00	1
$S_2$3e	483.50	8	134.22	1	6.50	4.73	109.31	0.816	91.13	0

Mol_MW: molecular weight; **#rotor:** No. of rotatable bonds; **donorHB:** No. of hydrogen bonds that would be donated by the solute to water molecules in an aqueous solution; **accptHB:** No. of hydrogen bonds that would be accepted by the solute from water molecules in an aqueous solution; **QPlogPo/w:** Predicted octanol/water partition coefficient; **QPPCaco:** Caco-2 cell permeability in nm/sec; **QPlogKhsa:** binding to human serum albumin; **Percentage Human-Oral Absorption:** human oral absorption on 0 to 100% scale; **PSA:** polar surface area; **Rule of Five:** No. of violations of Lipinski's rule of five.